Technical Report

TR-06-43

Earthquake induced rock shear through a deposition hole

Influence of shear plane inclination and location as well as buffer properties on the damage caused to the canister

Lennart Börgesson, Clay Technology AB

Jan Hernelind, 5T Engineering AB

October 2006

Svensk Kärnbränslehantering AB
Swedish Nuclear Fuel
and Waste Management Co
Box 5864
SE-102 40 Stockholm Sweden
Tel 08-459 84 00
+46 8 459 84 00
Fax 08-661 57 19
+46 8 661 57 19

Earthquake induced rock shear through a deposition hole

Influence of shear plane inclination and location as well as buffer properties on the damage caused to the canister

Lennart Börgesson, Clay Technology AB

Jan Hernelind, 5T Engineering AB

October 2006

Keywords: Earthquake, Buffer, Bentonite, Canister, Damage, Finite elements, Rock shear.

Abstract

The effect on the canister of an earthquake induced 20 cm rock shear with the shear rate 1 m/s along a fracture intersecting a deposition hole in a KBS-3V repository has been investigated for a number of different shear cases and for different properties of the buffer material. The scenarios have been modelled with the finite element method and calculations have been done using the code ABAQUS. 3D-element models of the rock, the buffer and the canister have been used. Contact elements that can model separation have been used for the interfaces between the buffer and the rock and the interfaces between the buffer and the canister.

The influence of mainly the following factors has been investigated:

1. Inclination of the intersecting fracture.
2. Shear direction when the fracture is not horizontal (inclination deviates from 90°).
3. Location of the shear plane when the inclination is 90°.
4. Magnitude of the shear displacement.
5. Bentonite type.
6. Bentonite density.
7. Transformation of the buffer to illite or cemented bentonite.

The results from the calculations show that all these factors have important influence on the damage of the canister but the influence is for most factors not easily described since there are mutual interferences between the different factors.

Plastic strain larger than 1% was reached in the copper already at 10 cm shear in all cases with Na- and Ca- bentonite. However, for several cases of Na-bentonite and one case of Ca-bentonite such plastic strain was only reached in the lid.

The plastic strain in the steel was generally smaller than in the copper mainly due to the higher yield stress in the steel. For all cases of Na-bentonite except one and for about half of the Ca-bentonite cases the plastic strain in the steel was smaller than 1% after 10 cm shear.

The shear inclination 45° was more harmful for the copper tube than the shear inclination 90° when tension shear was considered. At the shear inclinations 45° and 22.5° tension shear was always more harmful for the copper tube than compression shear. The highest value of the plastic strain in the copper tube was 19% and was reached after 20 cm shear in Ca-bentonite with the density 2,050 kg/m^3.

Higher plastic strain in the copper tube was at the shear angle 90° reached at eccentric shear than at centric shear for all cases except the high density Ca-bentonite case.

The plastic strain increased with increasing shear displacement although the influence of the shear displacement was reduced the softer the buffer material is.

The maximum plastic strain in the copper tube and in the iron insert was for all cases larger for the Ca-bentonite than for the Na-bentonite.

Conversion to illite yields that the effect on the canister of a rock shear is insignificant compared to when no transformation has taken place since the stiffness and strength of the illitic clay is only a tenth of the strength of MX-80, which in turn depends on that almost the entire swelling pressure is lost.

Cementation of bentonite with the thickness 8.75 cm around the canister yields that the effect of a rock shear is more severe than if the original bentonite is kept due to the increased stiffness of the buffer. However, the properties of cemented bentonite are not known so the calculation must be regarded as an example rather than as a prediction.

The plastic strains in the copper lids were in many cases rather large but by making a more optimized design it should be possible to reduce the strains.

The calculations are associated with several uncertainties that should be considered when the consequences of a rock shear are analyzed.

Sammanfattning

Inverkan av en jordbävningsinducerad 20 cm lång bergskjuvning med skjuvhastigheten 1 m/s längs en spricka genom ett deponeringshål i ett KBS-3V-förvar har undersökts för ett antal olika skjuvfall och för olika egenskaper hos buffertmaterialet. Scenarierna har modellerats med finita element metoden och beräkningarna gjorts med koden ABAQUS. En 3D elementmodell har använts för att modellera berg, buffert och kapsel. Kontaktelement som kan simulera separation har använts till kontaktytorna mellan buffert och berg och mellan buffert och kapsel.

Inverkan av i huvudsak följande faktorer har undersökts:

1. Lutningen hos den korsande sprickan.
2. Skjuvriktningen när sprickan inte är horisontell (lutningen avviker från 90°).
3. Skjuvplanets läge när lutningen är 90°.
4. Skjuvlängden.
5. Bentonitsort.
6. Bentonitdensitet.
7. Omvandling av bufferten till illit eller cementerad bentonit.

Resultaten från beräkningarna visar att alla dessa faktorer har stor inverkan på kapselns skada men inverkan är för de flesta fallen inte enkel att beskriva eftersom faktorerna påverkar varandra inbördes.

Plastiska töjningar större än 1 % uppkom i kopparn redan efter 10 cm skjuvning i alla fallen med Na- och Ca-bentonit. Men för ett flertal skjuvningar i Na-bentonit och en skjuvning i Ca-bentonit uppstod sådana plastiseringar endast i locket.

De plastiska töjningarna i stålet blev i regel mindre än i kopparn i huvudsak beroende på att flytspänningen är högre i stålet. För alla fallen med Na-bentonit utom en och för ungefär hälften av fallen med Ca-bentonit var de plastiska töjningarna i stålet mindre än 1 % efter 10 cm skjuvning.

Skjuvriktningen 45° var vid dragskjuvning skadligare för kopparn än skjuvriktningen 90°. Vid skjuvvinklarna 45° och 22,5° var alltid dragskjuvning farligare för kopparröret än tryckskjuvning. Det högsta värdet hos den plastiska töjningen i kopparröret var 19 % och uppnåddes efter 20 cm skjuvning i Ca-bentonit med densiteten 2 050 kg/m^3.

I kopparröret uppnåddes för alla fall med skjuvriktningen 90° större plastiska töjningar vid excentrisk skjuvning än vid centrisk skjuvning förutom för fallet med Ca-bentonit med den höga densiteten.

De plastiska töjningarna tycks öka med ökande skjuvrörelse fastän inflytandet av skjuvrörelsen minskar ju mjukare buffertmaterialet är.

De maximala plastiska töjningarna i kopparröret och stålinsatsen blev för alla fallen större med Ca-bentonit än med Na-bentonit.

Omvandling till illit medför att påverkan av en bergskjuvning på kapseln är obetydlig i jämförelse med när ingen omvandling skett eftersom styvheten och skjuvhållfastheten hos illitsk lera bara är en tiondel av de hos MX-80 vilket i sin tur beror på att nästa hela svälltrycket har tappats.

Cementerad bentonit med tjockleken 8,75 cm runt kapseln medför att påverkan av en bergskjuvning blir allvarligare än för den ursprungliga opåverkade bentoniten eftersom cementeringen ökar styvheten hos bufferten. Men egenskaperna hos cementerad bentonit är inte kända så den utförda beräkningen bör ses som ett exempel snarare än en prediktion.

Påkänningarna hos kopparlocken blev i många fall ganska stora men med en mer optimal utformning av locken bör det gå att minska dessa påkänningar radikalt.

Beräkningarna är förknippade med ett flertal osäkerheter som bör beaktas när konsekvenserna av en bergskjuvning analyseras.

Contents

1 Introduction

One important function of the buffer material in a deposition hole in a repository for nuclear waste disposal is to reduce the damage of rock movements on the canister. The worst case of rock movements is a very fast shear that takes place along a fracture and occurs as a result of an earthquake.

The consequences of such rock shear has been investigated earlier, both by laboratory tests (/1/ and /5/), laboratory simulations in the scale 1:10 /2/ and finite element modelling (/3/, /4/ and /5/).

Those investigations were only focussed on a base case with a horizontal shear plane and Na-bentonite as buffer material. Since it is very probable that the Na-bentonite will be transformed to Ca-bentonite or that Ca-bentonite might be used as buffer the calculations have been updated with new calculation using the material properties of Ca-bentonite instead of Na-bentonite.

The influence of the shear angle has not been investigated before so new models with 45 and 22.5 degrees inclination between the shear plane and the canister axis have been made and new calculations performed.

Transformation to illite or cementation of parts of the buffer may occur. The consequences of such transformations have been investigated. The effect of transformation to illite can easily be judged while the effect of cementation has been modelled with adopted cement properties for ¼ of the buffer.

2 Earlier investigations

The main investigations concerning rock shear through a deposition hole have been the following:

Model shear tests of a canister in a deposition hole

In this investigation /2/ a laboratory model in the scale 1:10 of a deposition hole with bentonite buffer and a canister was sheared with different shear rates. The canister was made of solid copper and it was surrounded by highly compacted water saturated MX-80 bentonite. Before shearing the swelling pressure was measured by six transducers in order to follow the water uptake process. During shearing pressure, strain, force and deformation were measured in altogether 18 points. The shearing was made at different rates in the various tests.

An extensive sampling after shear was made and the density, water content, degree of saturation, homogenisation and the effect of shear on the bentonite and canister were measured and studied. The results from the shear tests were compared to different calculations. The relevance of the calculations and the need for improved mathematical models could then be studied.

One important conclusion from these tests was that the rate dependence is about 10% increased shear resistance per decade of increased rate of shear. This resulted also in a very clear increase in strain in the canister with increased rate. The results also showed that the saturated bentonite has excellent stress distributing properties. However, the high density of the clay (ρ_m = 2,050 kg/m^3) made the bentonite produce such a high swelling pressure that the material was rather stiff resulting in a strong deformation of the canister. Since the canister was made of solid copper, it was deformed more than would be expected from a canister with a cast iron insert.

Finite element calculations for evaluating the material model and investigate the influence of different factors

The model test was simulated in finite element calculations with the purpose to check the reliability of the material models and the calculation technique and to investigate the influence of some factors /3/. Good agreement between calculated and measured results was reached and it was concluded that the elasto-plastic material model was relevant for this type of fast shear. It was also concluded that the buffer was completely plasticized around the influenced parts of the canister and that the influence of buffer thickness was small but the influence of density large.

Finite element calculations for investigating the mechanical interaction between bentonite buffer and the canister in a deposition hole

The function of the bentonite buffer as a mechanical protection of the canister in a repository was investigated in a number of finite element calculations /4/. Three canister types (KBS3 HIP canister, KBS3 Cu/Fe composite canister and VLH large canister) and two repository concepts (KBS3 and VLH) were compared.

The functions and scenarios were simulated by the finite element code ABAQUS. The bentonite was modelled with the effective stress theory with Porous Elasticity and Drucker Prager Plasticity according to a model derived from laboratory investigations.

The most important results from the calculations were the following:

The water and swelling pressure will close the gap between the copper and the cast iron in the composite canisters except at the edges of the lids when the canister has flat ends.

A rock displacement of 10 cm across the deposition hole will cause some plastic strain in the copper in all concepts and for all canisters investigated but the plastic strain will be small with a maximum of 4% which was achieved at a density higher than intended for actual use in repositories.

Laboratory tests for investigating the influence of shear rate on shear strength

The shear strength of MX-80, which is the main buffer property required for the rock shear calculation, was measured in a number of shear tests with shear rates varying from 0.025 to 25% per hour corresponding to about $3 \cdot 10^{-9}$ to $3 \cdot 10^{-6}$ m/s /1/. These rather slow tests showed that the shear strength increased linearly with shear rate in a double logarithmic scale. The increase was 16% per 10 times increased shear rate.

A large number of additional very fast laboratory shear tests were performed in order to investigate the influence of the shear rate on the shear strength /5/. These tests, which were done with shear rates up to more than 1 m/s, confirmed the values of the shear strength for some of the relevant densities.

The influence of the bentonite buffer density is much stronger than the influence of the shear rate. In order to reach the same influence on the buffer shear strength as a ten times increase in shear rate the density must be increased with about 15 kg/m^3 or 0.75%.

Calculations for investigating of the influence of shear rate, buffer density, shear displacement and the location of the horizontal shear plane

This investigation /5/ yielded the following main results and conclusions:

The calculations were done with an assumed shear rate of 1.0 m/s at the buffer densities 1,950, 2,000, 2,050 and 2,100 kg/m^3. At the reference case (density 2,000 kg/m^3 and eccentric shear) the plastic strain in the cast iron insert started after 2 cm shear and increased to 4.4% plastic strain after 20 cm shear displacement. The corresponding maximum plastic strain in the copper was about 8% on the canister envelope surface while it was locally much higher at the lid.

The influence of buffer density is very strong and an increase in density from the reference case (eccentric shear) 2,000 kg/m^3 to 2,100 kg/m^3 yielded an increase in plastic strain after 20 cm displacement from 4.4% to 10%, while a reduction in density to 1,950 yielded a reduction in plastic strain to 2.7%.

There was also a surprisingly strong influence of the shear plane location. For centric shear at the buffer densities 1,950 and 2,000 kg/m^3 there was practically no plasticization of the cast iron insert, while at the higher densities 2,050 and 2,100 kg/m^3 the plastic strain was 11% and 19% respectively. The influence of buffer density was thus much stronger at centric shear than at eccentric shear. The reason is judged to be that at low density a long part of the canister is needed for keeping it in a firm grip strong enough to prevent tilting, which means that one side of the canister is prevented from tilting at the eccentric shear while the whole canister tilts at centric shear. The reverse is the case at high density where the length of the canister is enough to keep both ends in a firm grip at centric shear and prevent both end from tilting, while the shorter part of the canister still can tilt at the eccentric shear.

The influence of the magnitude of the shear displacement logically seemed to be rather strong when the canister was prevented from tilting with a plastic strain that usually was more than doubled at an increase in shear displacement from 10 cm to 20 cm. However, when the buffer plasticized at a shear strength that was not high enough to prevent tilting the magnitude of the shear displacement had no effect, since the canister just continued to tilt as in a liquid with high viscosity.

The copper canister was strongly plasticized according to these calculations especially at the high densities. In contrast to the cast iron insert the copper was not affected by the shear plane location. However, the copper was strongly influenced by the tension stresses on the passive sides. When a more realistic model with contact elements was used the plasticization of the copper was reduced to the same magnitude as in the cast iron insert for the reference case.

The plastic strain in the cast iron was, in contrary to the copper, not affected by introducing contact elements around the copper canister due to the slot between the copper and the cast iron, which has the same effect for the cast iron as the contact elements for the copper.

3 FE-program and material models

3.1 General

The finite element code ABAQUS was used for the calculations. ABAQUS contains a capability of modelling a large range of processes in many different materials as well as complicated three-dimensional geometry. The code includes special material models for rock and soil and ability to model geological formations with infinite boundaries and in situ stresses by e.g. the own weight of the medium. Detailed information of the available models, application of the code and the theoretical background are given in the ABAQUS manuals /6/.

3.2 Material models

3.2.1 General

Three materials have been modelled. The copper canister and the cast iron insert have properties mainly taken from /5/ and these properties are the same in all calculations. For the bentonite buffer three different models have been used, one for Na-bentonite, one for Ca-bentonite and one for the cemented part of the bentonite.

3.2.2 Bentonite buffer

The bentonite buffer is modelled using only total stresses that don't include the pore water pressure, the reason being the very fast compression and shear. The stress-strain relation is in ABAQUS described with von Mises stress σ_j that describes the "shear stress" in three dimensions according to Equation 3-1.

$$\sigma_j = (((\sigma_1 - \sigma_3)^2 + (\sigma_1 - \sigma_2)^2 + (\sigma_2 - \sigma_3)^2)/2)^{1/2} \quad (3\text{-}1)$$

where

σ_1, σ_2 and σ_3 are the major principal stresses.

At triaxial tests σ_2 and σ_3 are equal and the Mises stress equal to the deviator stress q.

$$q = (\sigma_1 - \sigma_3) \quad (3\text{-}2)$$

The model includes an elastic part and a plastic part. Equations 3-2 to 3-4 are used for defining the shear strength and the influence of density, pressure and rate of shear /5/.

Relation between swelling pressure and void ratio

The relation between swelling pressure and void ratio can be described according to Equation 3-2:

$$p = p_0 \left(\frac{e}{e_0} \right)^{\frac{1}{\beta}} \quad (3\text{-}2)$$

where

e = void ratio

e_0 = reference void ratio (= 1.1)

p = swelling pressure (at e)

p_0 = reference swelling pressure (at e_0) (= 1,000 kPa)

β = –0.19

e_0, p_0 and β are derived for MX-80.

Relation between shear strength and swelling pressure

The relation between shear strength (or deviator stress at failure) and swelling pressure can be described according to Equation 3-3:

$$q_f = q_{f0}\left(\frac{p}{p_0}\right)^b \tag{3-3}$$

where

q_f = deviator stress at failure at the swelling pressure p

q_{f0} = 500 kPa (deviator stress at failure at the swelling pressure p_0)

p_0 = 1,000 kPa

b = 0.77

The parameter values are based on triaxial tests on MX-80 with the very low shear rate $v_s = 5 \cdot 10^{-5}$ mm/s.

Relation between shear strength and shear rate

The relation between shear strength and shear rate can be described according to Equation 3-4:

$$q_{fs} = q_{fs0}\left(\frac{v_s}{v_{s0}}\right)^n \tag{3-4}$$

where

v_s = shear rate

v_{s0} = reference shear rate

q_{fs} = deviator stress at failure at the shear rate v_s

q_{fs0} = deviator stress at failure at the reference shear rate v_{s0}

n = 0.065

The value n=0.065 was found for MX-80 at low shear rates and verified by tests with shear rates up to 1 m/s /5/.

The buffer properties described by Equations 3-2 to 3-4 are thus evaluated for the Na-bentonite MX-80. The parameters derived are not valid for Ca-bentonite.

The results are thus only valid for MX-80 sodium bentonite. If another bentonite type is used or if a geochemical transformation of the buffer takes place the properties described by Equations 3-2 and 3-3 will be different. Tests on Ca-bentonite show that both the swelling pressure and the strength of a Ca-bentonite are higher than for a Na-bentonite (see Figure 3-1). A transformation to Ca-bentonite would thus according to these results probably also yield an increase in swelling pressure. At the density at saturation ρ = 2,000 kg/m^3 (or the void ratio e = 0.78) the swelling pressure increases from ~ 6.1 MPa to ~ 12 MPa, corresponding to an increase with a factor of about 2. The maximum deviator stress q_f that the buffer can withstand increases from ~ 2 MPa (at the swelling pressure of MX-80 of 6 MPa) to ~ 5.1 MPa (at the swelling pressure of Ca-bentonite of 12 MPa). At the density at saturation ρ = 2,100 kg/m^3 (or the void ratio e=0.69) the corresponding swelling pressure of Ca-bentonite is about 25 MPa and the maximum deviator stress about 9 MPa.

The additional increase in shear strength caused by the high shear rate is according to Equation 3-4 a factor 2.98 when the shear rate is increased from the shear rate $v_s = 5 \cdot 10^{-8}$ m/s used in the triaxial tests to the maximum shear rate v_s = 1.0 m/s expected at an earthquake. The same relation is assumed to be valid for Ca-bentonite.

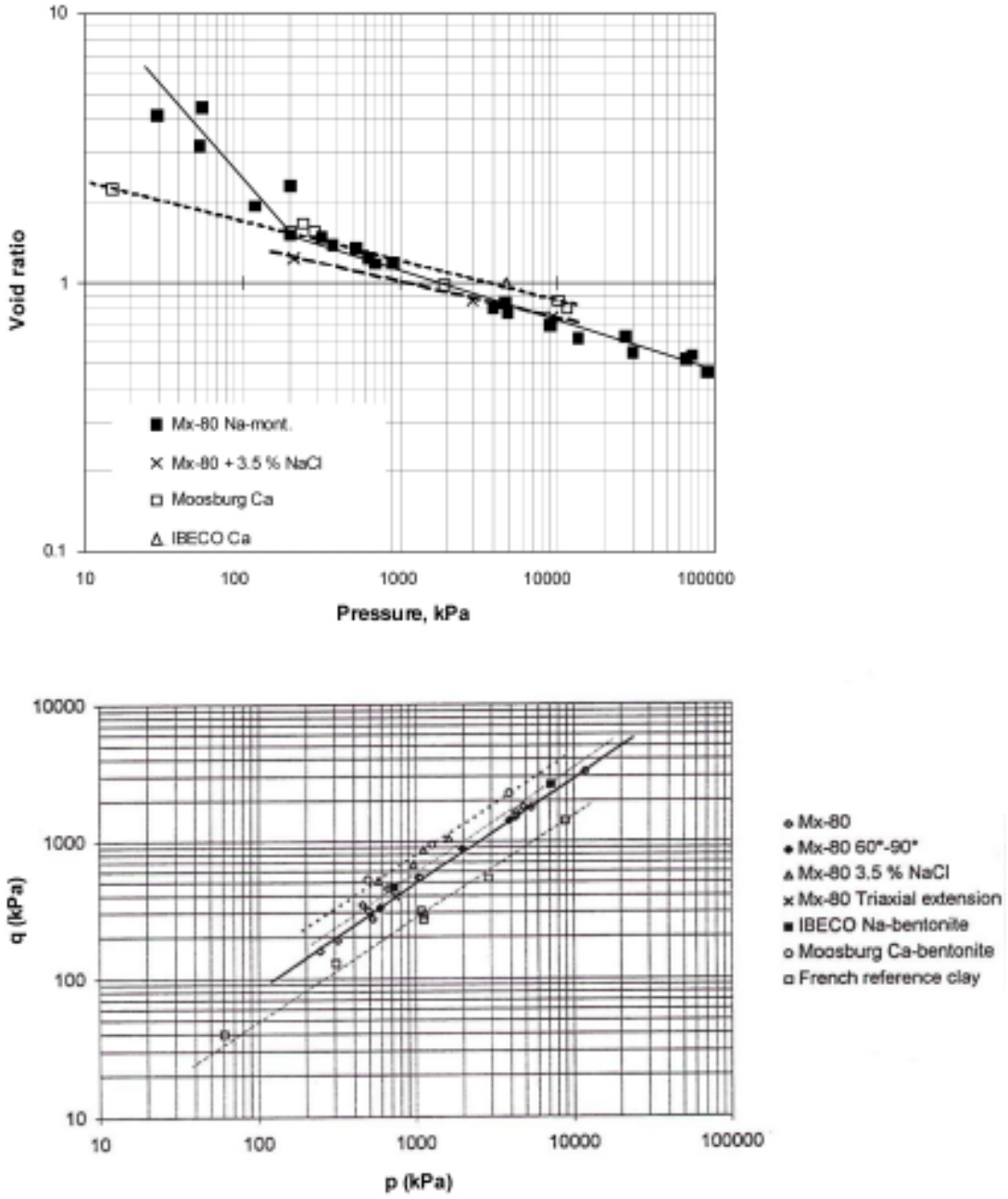

Figure 3-1. *Measured relations between swelling pressure and void ratio (upper) and between deviatoric strength* ***q*** *and swelling pressure* ***p*** *for different bentonite types /7/.*

Table 3-1 shows the values used for the different materials.

Table 3-1. Swelling pressure *p* and maximum deviator stress q_f for Na- and Ca-bentonite buffer used in the rock shear calculations.

Material	ρ_m kg/m³	*e*	*p* MPa)	q_f (MPa) at $v_s = 5{\cdot}10^{-8}$ m/s	q_{fs} (MPa) at v_s = 1.0 m/s
Na-bentonite	2,000	0.78	6.1	2.0	6.0
Na-bentonite	2,050	0.69	11.6	3.3	10.0
Ca-bentonite	2,000	0.78	12.0	5.1	15.2
Ca-bentonite	2,050	0.69	25.0	9.0	26.8

In addition to the maximum deviator stress the elastic parameters E and v and the plastic strain relation are needed. For Na-bentonite those relations were derived from the results of the laboratory tests /5/. The same type of relation is valid for Ca-bentonite.

Table 3-2 shows the elastic and plastic data for the four materials.

The relations between Mises stress and engineering strain for all four bentonite cases are shown in Figure 3-2.

3.2.3 Cemented bentonite buffer

General

The model is a continuum, plasticity-based, damage model for concrete /6/. It assumes that the main two failure mechanisms are tensile cracking and compressive crushing of the concrete material. The evolution of the yield (or failure) surface is controlled by two hardening variables, $\tilde{\varepsilon}_t^{pl}$ and $\tilde{\varepsilon}_c^{pl}$, linked to failure mechanisms under tension and compression loading, respectively. $\tilde{\varepsilon}_t^{pl}$ and $\tilde{\varepsilon}_c^{pl}$ is referred to as tensile and compressive equivalent plastic strains, respectively. The following sections discuss the main assumptions about the mechanical behaviour of concrete.

Uniaxial tension and compression stress behaviour

The model assumes that the uniaxial tensile and compressive response of concrete is characterized by damaged plasticity, as shown in Figure 3-3.

Table 3-2. Elastic-plastic material data for the bentonite buffer.

Material	ρ_m kg/m³	Elastic part E MPa	v	Plastic part: von Mises stress σ_j (MPa) at the following plastic strains ε_p ε_p = 0	ε_p = 0.002	ε_p = 0.005	ε_p = 0.009	ε_p = 0.013	ε_p = 0.018	ε_p = 0.023	ε_p = 1.0
Na-b	2,000	363	0.49	3.63	4.85	5.57	5.95	6.19	6.3	6.22	6.22
Na-b	2,050	583	0.49	5.83	7.77	8.93	9.53	9.92	10.1	9.97	9.97
Ca-b	2,000	865	0.49	8.65	11.54	13.27	14.15	14.73	15.0	14.81	14.81
Ca-b	2,050	1,525	0.49	15.25	20.35	23.40	24.95	25.97	26.45	26.11	26.11

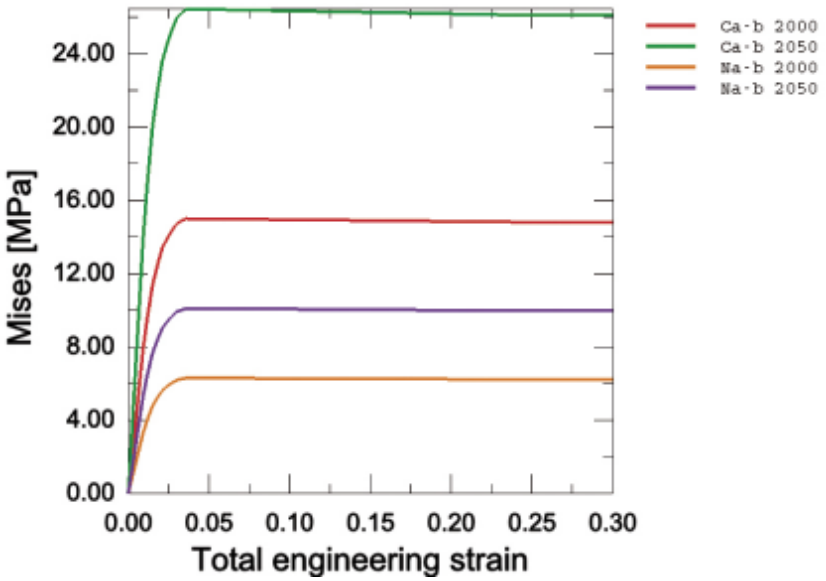

Figure 3-2. *Mises stress (kPa) as function of strain for the four bentonite materials at the shear rate 1 m/s.*

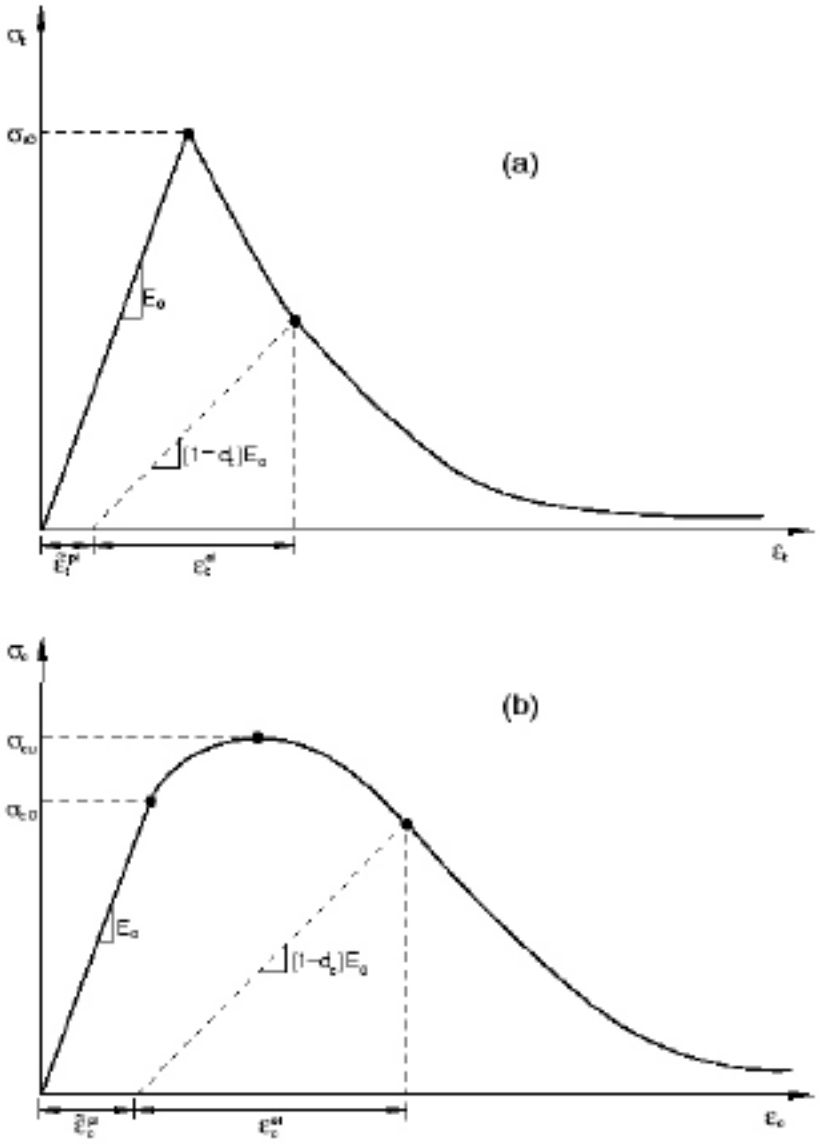

Figure 3-3. *Response of concrete to uniaxial loading in tension (a) and compression (b).*

Under uniaxial tension the stress-strain response follows a linear elastic relationship until the value of the failure stress, σ_{t0}, is reached. The failure stress corresponds to the onset of micro-cracking in the concrete material. Beyond the failure stress the formation of micro-cracks is represented macroscopically with a softening stress-strain response, which induces strain localization in the concrete structure. Under uniaxial compression the response is linear until the value of initial yield, σ_{c0}. In the plastic regime the response is typically characterized by stress hardening followed by strain softening beyond the ultimate stress, σ_{cu}. This representation, although somewhat simplified, captures the main features of the response of concrete.

It is assumed that the uniaxial stress-strain curves can be converted into stress versus plastic-strain curves. (This conversion is performed automatically by ABAQUS from the user-provided stress versus "inelastic" strain data, as explained below.) Thus,

$\sigma_t = \sigma_t (\tilde{\varepsilon}_t^{pl}, \dot{\tilde{\varepsilon}}_t^{pl}, \theta, f_i)$,

$\sigma_c = \sigma_c (\tilde{\varepsilon}_c^{pl}, \dot{\tilde{\varepsilon}}_c^{pl}, \theta, f_i)$,

where the subscripts t and c refer to tension and compression, respectively; $\tilde{\varepsilon}_t^{pl}$ and $\tilde{\varepsilon}_c^{pl}$ are the equivalent plastic strains, $\dot{\tilde{\varepsilon}}_t^{pl}$ and $\dot{\tilde{\varepsilon}}_c^{pl}$ are the equivalent plastic strain rates, θ is the temperature, and f_i, (i = 1, 2, ...) are other predefined field variables.

As shown in Figure 3-3, when the concrete specimen is unloaded from any point on the strain softening branch of the stress-strain curves, the unloading response is weakened: the elastic stiffness of the material appears to be damaged (or degraded). The degradation of the elastic stiffness is characterized by two damage variables, d_t and d_c, which are assumed to be functions of the plastic strains, temperature, and field variables:

$d_t = d_t\,(\tilde{\varepsilon}_t^{pl},\ \theta, f_i); \quad 0 \le d_t \le 1,$

$d_c = d_c\,(\tilde{\varepsilon}_c^{pl},\ \theta, f_i); \quad 0 \le d_c \le 1.$

The damage variables can take values from zero, representing the undamaged material, to one, which represents total loss of strength.

If E_0 is the initial (undamaged) elastic stiffness of the material, the stress-strain relations under uniaxial tension and compression loading are, respectively:

$\sigma_t = (1-d_t)\,E_0(\varepsilon_t - \tilde{\varepsilon}_t^{pl}),$

$\sigma_c = (1-d_c)E_0(\varepsilon_c - \tilde{\varepsilon}_c^{pl}).$

We define the "effective" tensile and compressive cohesion stresses as

$$\sigma_t = \frac{\sigma_t}{(1-d_t)} = E_0(\varepsilon_t - \tilde{\varepsilon}_t^{pl}),$$

$$\sigma_c = \frac{\sigma_c}{(1-d_c)} = E_0(\varepsilon_c - \tilde{\varepsilon}_c^{pl}).$$

The effective cohesion stresses determine the size of the yield (or failure) surface.

An example of a load cycle with at first tension and then compression is shown in Figure 3-4.

Parameter values used for cemented buffer

Elastic part

The following E-modulus and Poisson's ratio have been used

E = 36,300 MPa

v = 0.3

Plastic part

The input data is rather complicated and only a brief explanation will be given. Several sets of plastic damage parameters are required:

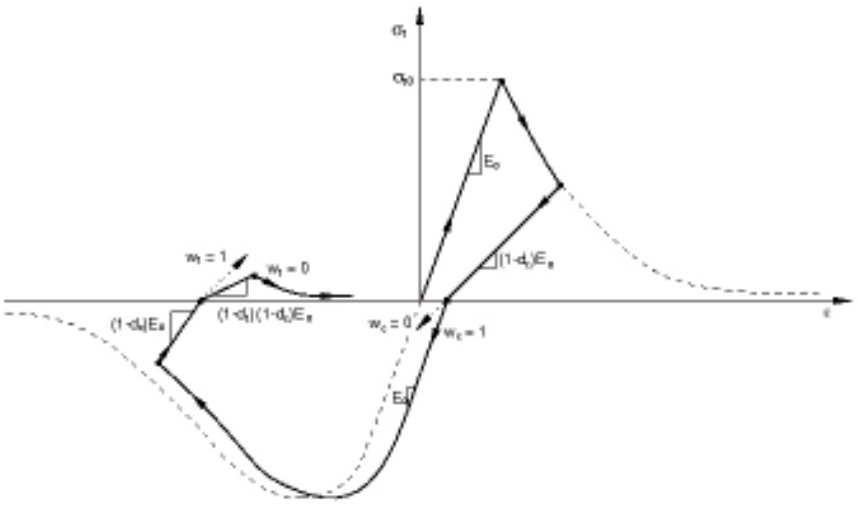

Figure 3-4. *Uniaxial load cycle (tension-compression-tension) assuming default values for the stiffness recovery factors:* $w_t = 0$ *and* $w_c = 1$.

Concrete Damage Plasticity

5 parameters need to be settled:

2.0; 0.2; 1.01; 1.0; 0

The first parameter is the dilation angle, the second parameter is the flow potential eccentricity, the third parameter is the ratio of equibiaxial compressive yield stress to initial uniaxial compressive yield stress, the fourth parameter is the ratio of the second stress invariant on the tensile meridian and the last one is a viscosity parameter.

Concrete Compression Hardening

The yield curve at compression needs to be defined:

Table 3-3. Yield curve at compression.

Mises stress (MPa)	Compr strain
25	0
30	0.01
20	0.02
2	0.05
0.1	0.1
0.01	0.2
0.001	0.3

Concrete Tension Stiffening

Also the yield curve at tension needs to be defined:

Table 3-4. Yield curve at tension.

Mises stress (MPa)	Tension strain
5	0
0.1	0.01
0.01	0.015

Concrete compression damage

The parameter d_c that defines the elastic response at unloading (see Figure 3-4) needs to be settled if it deviates from zero:

Table 3-5. d_c as function of plastic strain.

d_c	Plastic strain
0	0
0.1	0.01
0.2	0.02
0.5	0.05
0.8	0.3
0.9	0.5

3.2.4 Cast iron and copper in the canister

The properties of the copper canister and the cast iron insert are also modelled with an elastic plastic model of the Mises stresses with identical properties as used in the former report /5/. Table 3-6 and Figure 3-5 show the relations.

3.2.5 Rock

In contrast to the former calculation /5/ the rock has been included in the new calculations on the following reasons:

1. The model has been improved with contact elements between the rock and the buffer and in order to use contact elements they must adjoin elements on both sides (thus both rock and buffer elements).
2. The shear direction is more easily modelled when it is defined with an outer structure.

The rock has been modelled as elastic and so stiff that the properties do not influence the results, i.e. the possible real influence of the rock stiffness has not been considered since it is very high in comparison to the buffer.

Table 3-6. Elastic-plastic material data for the copper and cast iron.

Material	Elastic part		Plastic part: von Mises stress σ_j (MPa) at the following plastic strains ε_p			
	E MPa	v	$\varepsilon_p = 0$	$\varepsilon_p = 0.2$	$\varepsilon_p = 0.5$	$\varepsilon_p = 1.0$
Copper	$1.2 \cdot 10^5$	0.33	50	–	200	200
Cast iron	$1.5 \cdot 10^5$	0.32	260	400	–	400

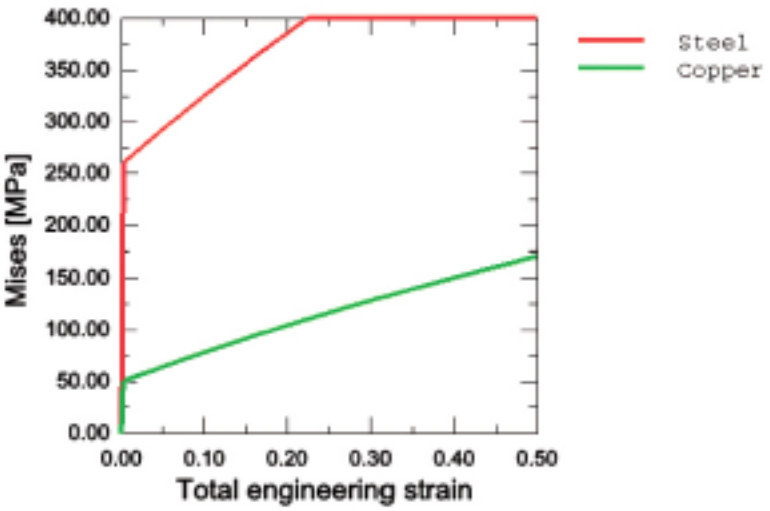

Figure 3-5. *Mises stress (kPa) as function of strain for copper and cast iron.*

4 Influence of shear angle and bentonite type on the damage of the canister

4.1 General

The calculations with Na- and Ca- bentonite as buffer materials have focussed on investigating the influence of the following variables on the damage of the canister:

- Bentonite type (Na or Ca)
- Shear angle (22.5, 45 and 90 degrees angle to the canister axis)
- Buffer density at saturation (2,000 and 2,050 kg/m^3)
- Shear displacement (10 and 20 cm)

In addition the direction of the shear has been changed for the models with 22.5 and 45 degrees shear angle and the location of the shear plane has been varied for the model with 90 degrees shear angle.

4.2 Element mesh

Four different element models have been used, one for each shear angle and one additional with eccentric shear for the model with 90 degrees shear angle.

Figure 4-1 shows the mesh of two of the 3D models as examples. The models have been tilted 90° and the rock and buffer located to the left of the shear plane have been removed from the models for illustration. The models are symmetric along the axial plane that cuts the deposition hole into two halves. The insert is of the BWR type with 12 channels for fuel assemblies. The dimensions are the following:

- Deposition hole: diameter 1.75 m and length 6.835 m.
- Copper canister: outer diameter 1.05 m and outer length 4.835 m.
- Copper wall thickness: 0.05 m.
- Cast iron insert: diameter 0.949 m and length 4.733 m.
- Wall thickness between fuel assemblies: 0.05 m.

A 0.5 mm slot between the copper canister and the cast iron insert is thus included in the model.

The model also includes contact elements on all bentonite surfaces, i.e. all contacts between the buffer and the rock and between the buffer and the copper canister. There are also contact elements in the slot between the copper and steel. All contact elements have friction at sliding along the elements with no cohesion and the friction coefficient 0.1, i.e. the friction angle and cohesion are

$\varphi = 5.7°$

$c = 0$ kPa

The model used in the earlier calculations /5/ has thus been improved since most of the old calculations were done with the bentonite tied to the rock and the canister. The consequence of using contact elements is reduced stresses in the buffer and in the canister. This is judged to better simulate the real case although the assumption of no cohesion yielding that the contact is released when the swelling pressure is lost should be checked in the laboratory.

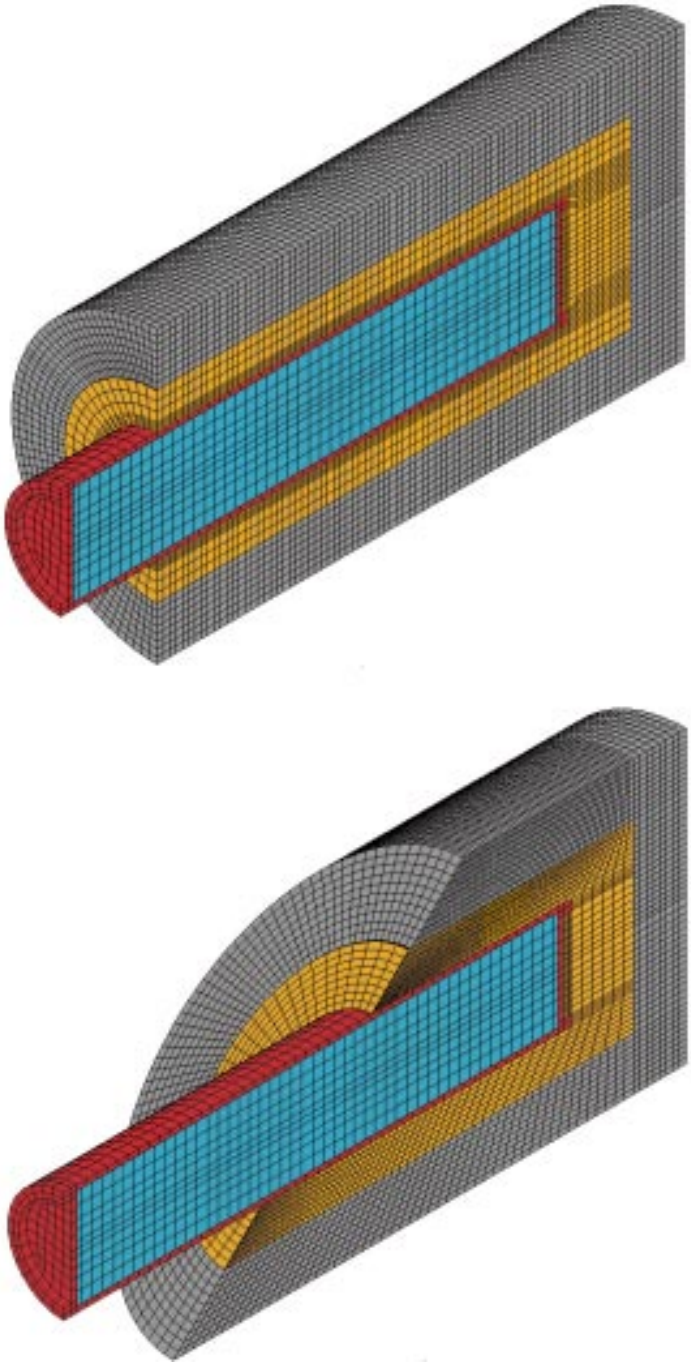

Figure 4-1. *Element mesh (tilted 90°) for two of the models with all the rock and bentonite located on one side of the shear plane removed. Upper figure: 90° shear angle and eccentric shear. Lower figure: 45° shear angle). Grey: rock. Orange: bentonite. Red: copper. Light blue: steel.*

4.3 Modelling sequence and extent

The calculations have been done in two steps. At first the swelling pressure has been applied, which mainly has resulted in a deformation of the copper canister due to the closure of the 1 mm gap between the copper and cast iron. Then the shear has started and continued until a total shear displacement of 20 cm.

Altogether 24 calculations have been performed; 12 on each bentonite type of which 4 calculations were done on each of the three shear angles. At the shear angle 90° two different shear locations were used (centric and eccentric) and for the shear angles 22.5° and 45° two

shear directions need to be modelled since there is a large difference if the shear implies a compression or extension of the deposition hole. The two cases are illustrated in Figure 4-2. The two densities at saturation ρ = 2,000 kg/m^3 and ρ = 2,050 kg/m^3 were simulated for all cases.

4.4 Results

The results of all 24 calculations are summarised in Tables 4-1 and 4-2, which show the maximum plastic strain in the copper tube, the copper lid and the cast iron insert after 10 cm and 20 cm rock displacement. The copper lid is defined as the end parts of the copper canister and 5–10 cm of the adjoining tube.

Table 4-1. Plastic strain in the canister after a rock shear through a deposition hole with a buffer of Ca-bentonite.

Calculation	ρ_m kg/m^3	Shear angle °	Shear direction/ location	Maximum plastic strain (%) After 10 cm shear			After 20 cm shear		
				Cu-tube	Cu-lid	Fe-insert	Cu-tube	Cu-lid	Fe-insert
Shear 22c5	2,000	22.5	Comp.	0.4	15	<1	0.6	27	2.8
Shear 22c7	2,000	22.5	Tension	4.4	2.5	<1	6	7.7	<1
Shear 22c6	2,050	22.5	Comp.	1.0	19	3.6	2.5	32	11
Shear 22c8	2,050	22.5	Tension	6.4	2	<1	10	6	1.5
Shear 45c5	2,000	45	Comp.	1.5	16	<1	2.0	29	2.9
Shear 45c7	2,000	45	Tension	7.5	5	<1	11	8	1.4
Shear 45c8	2,050	45	Comp.	4.5	13	1.7	10	20	5.9
Shear 45c6	2,050	45	Tension	10	4	<1	19	6	4
Shear 90c5_c	2,000	90	Centric	1.2	4.7	<1	2.5	8.0	1.5
Shear 90c5	2,000	90	Excentr.	2.5	3.4	2.3	6.5	7	4.9
Shear 90c6_c	2,050	90	Centric	7.2	2.0	5.4	16	3.0	13
Shear 90c6	2,050	90	Excentr.	5.5	5	2.4	13.5	9	7

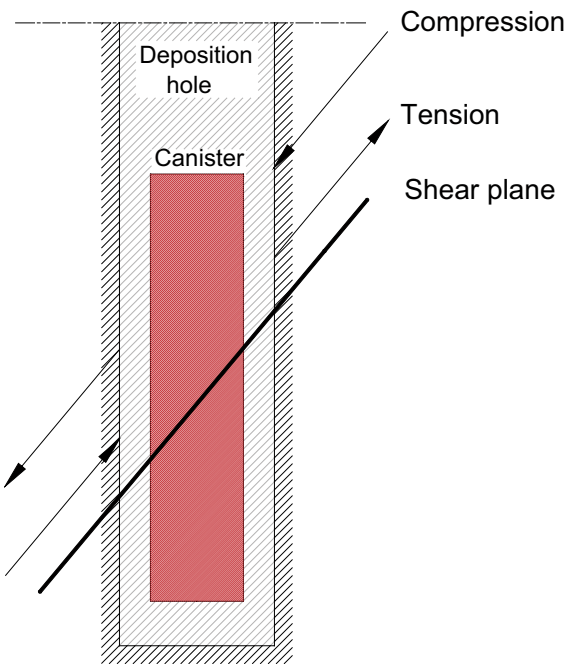

Figure 4-2. *Illustration of the difference between compression and tension during shear.*

Table 4-2. Plastic strain in the canister after a rock shear through a deposition hole with a buffer of Na-bentonite.

Calculation	ρ_m kg/m³	Shear angle °	Shear direction/ location	Maximum plastic strain (%) After 10 cm shear			After 20 cm shear		
				Cu-tube	Cu-lid	Fe-insert	Cu-tube	Cu-lid	Fe-insert
Shear 22c1	2,000	22.5	Comp.	0.2	6.8	<1	0.3	13	<1
Shear 22c2	2,000	22.5	Tension	2.5	3.5	<1	3.3	7.8	<1
Shear 22c3	2,050	22.5	Comp.	0.3	12	<1	0.4	21	<1
Shear 22c4	2,050	22.5	Tension	3.5	3.8	<1	4.6	10	<1
Shear 45c1	2,000	45	Comp.	0.5	10	<1	0.6	15	<1
Shear 45c2	2,000	45	Tension	3.5	3.8[1)]	<1	5.0	7.6	<1
Shear 45c3	2,050	45	Comp.	0.8	15	<1	1.5	23	<1
Shear 45c4	2,050	45	Tension	5.5	5.0[1)]	<1	8	8	<1
Shear 90c1_c	2,000	90	Centric	0.2	2.1	<1	0.3	4.3	<1
Shear 90c1	2,000	90	Excentr.	1.2	7.9	<1	2.0	11	1.7
Shear 90c3_c	2,050	90	Centric	0.4	3.7	<1	0.5	6.7	<1
Shear 90c3	2,050	90	Excentr.	1.2	7.8	1.3	2.5	13	3.6

1) About 10 cm from the lid.

A number of examples of results are shown in Figures 4-3 to 4-12.

Figures 4-3 to 4-5 show some results of calculation *Shear 45c6* where tension shear at the inclination 45° occurs through a deposition hole filled with Ca-bentonite with the density 2,050 kg/m³. Figure 4-3 shows that the peak strength of the buffer (plastic strain ≈ 5%) has been reached for a zone 0.5–1 m around the shear plane and that the average stress is higher than the swelling pressure (25 MPa) in almost the entire buffer after 20 cm shear. Only the bentonite close to the lids has a reduced stress. Figure 4-4 shows the deformed canister after 10 and 20 cm displacement. The shape of the canister shows that the steel insert is bent and not tilted and that the copper tube is clearly exposed to tension since the lid is buckled inwards. Figure 4-5 shows the plastic strain in the copper and steel. The canister is plasticized in a zone around the shear plane and the plastic strain reaches almost 20% locally in the copper while it is only a few per cent in the steel.

Figures 4-6 and 4-7 show some results of calculation *Shear 90c6_c* where centric shear with the inclination 90° towards the hole axis occurs through a deposition hole filled with Ca-bentonite with the density 2,050 kg/m³. Figure 4-6 shows the consequences for the buffer. The bentonite between the canister and the rock close to the shear plane has come off from both the rock and the canister and formed open slots at the passive parts. The figure also shows that the plastic strain in the buffer is higher than 5% at a zone around the shear plane that is even narrower than for the previously shown calculation (*shear 45c6*) while the buffer around the ends of the canister has very small or no plastic strain yielding that the canister is kept in a firm grip. Just as for the 45° shear the net average stress is positive (higher than the swelling pressure 25 MPa) for a major part of the buffer but unlike the 45° shear there is a reduction in pressure on the passive side of the canister. The plastic strain in the copper shown in Figure 4-7 is concentrated to a rather small area in the centre of the canister and amounts at maximum to about 16%. The plastic strain in the steel is also very high and at maximum almost 13%. The rather strong bending of the canister is clearly seen even in these figures with no magnification of the displacements.

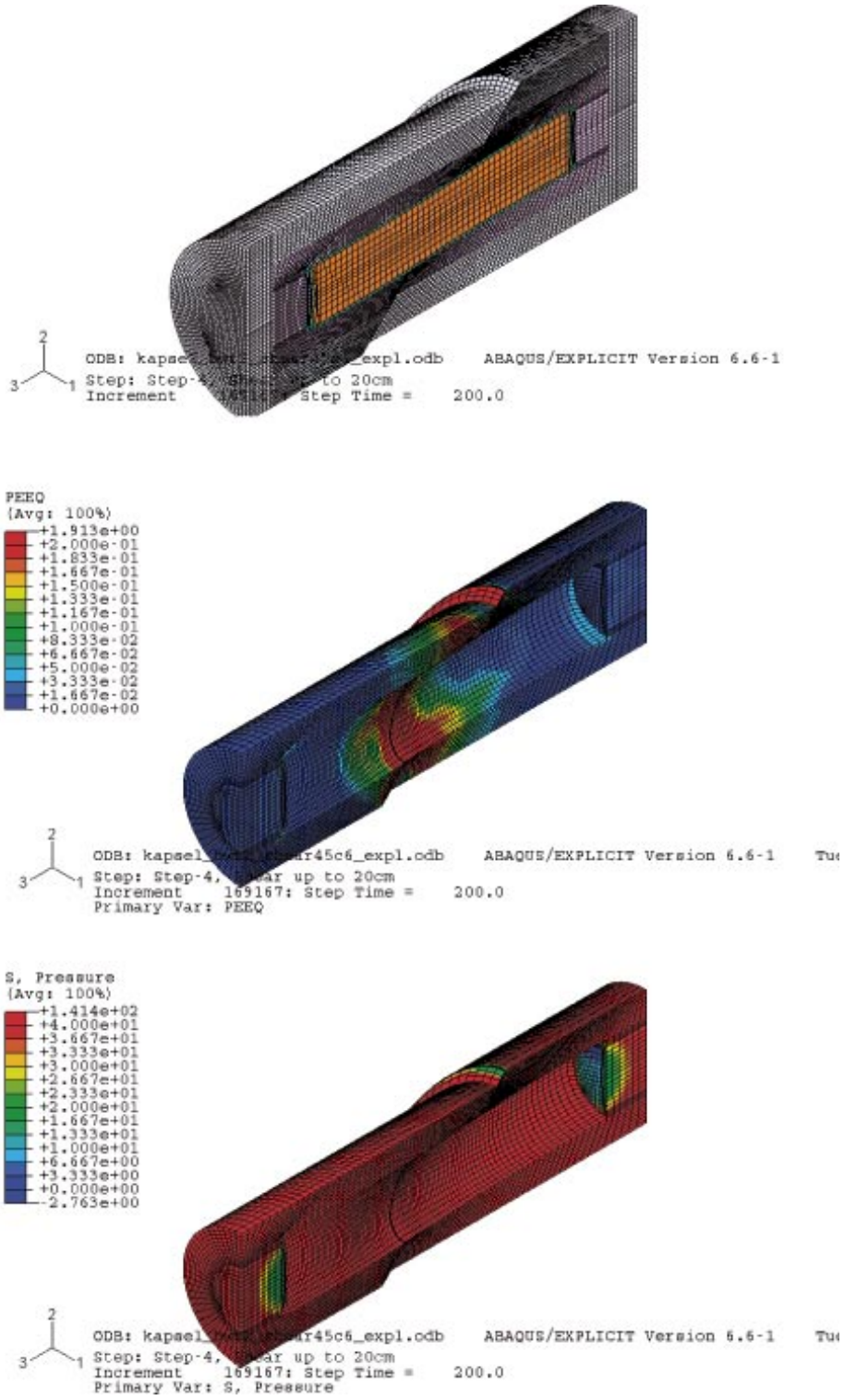

Figure 4-3. *Shear 45c6; Ca-bentonite; ρ_m = 2,050 kg/m^3; 45° tension shear. Results after 20 cm shear. Deformed entire mesh, plastic strain and average stress (MPa) in the bentonite.*

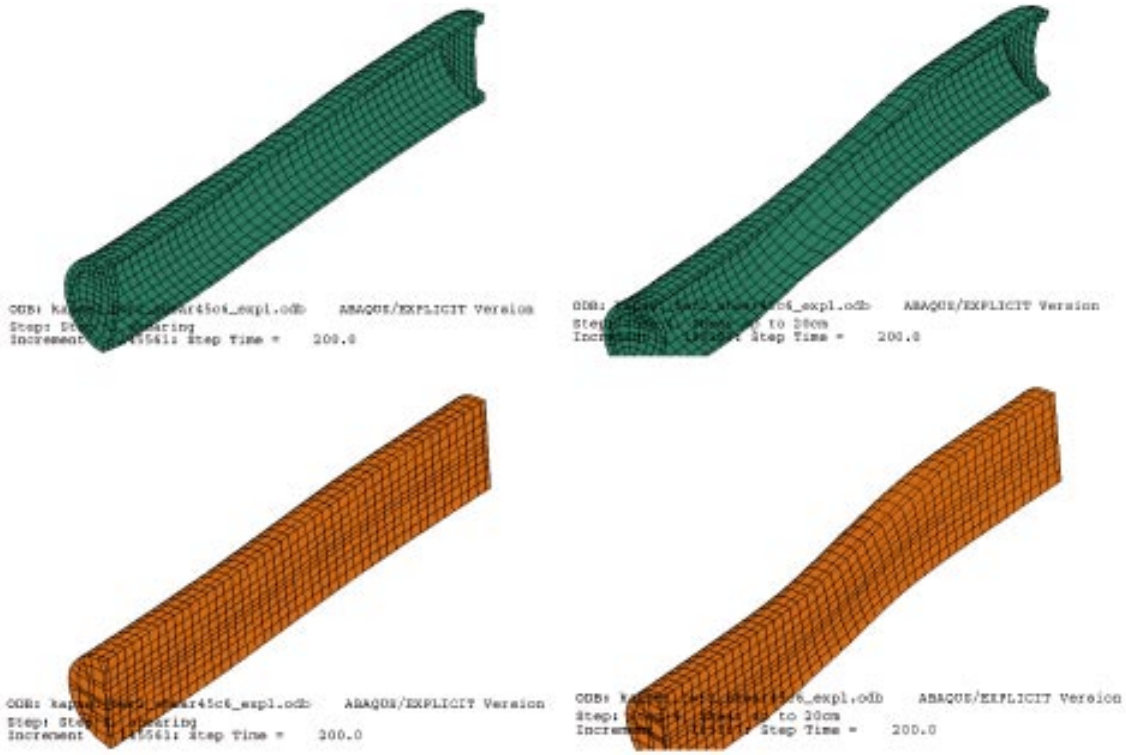

Figure 4-4. *Shear 45c6; Ca-bentonite; ρ_m = 2,050 kg/m³; 45° tension shear. Deformed copper and steel parts after 10 cm and 20 cm displacement. Deformations are magnified a factor 5.*

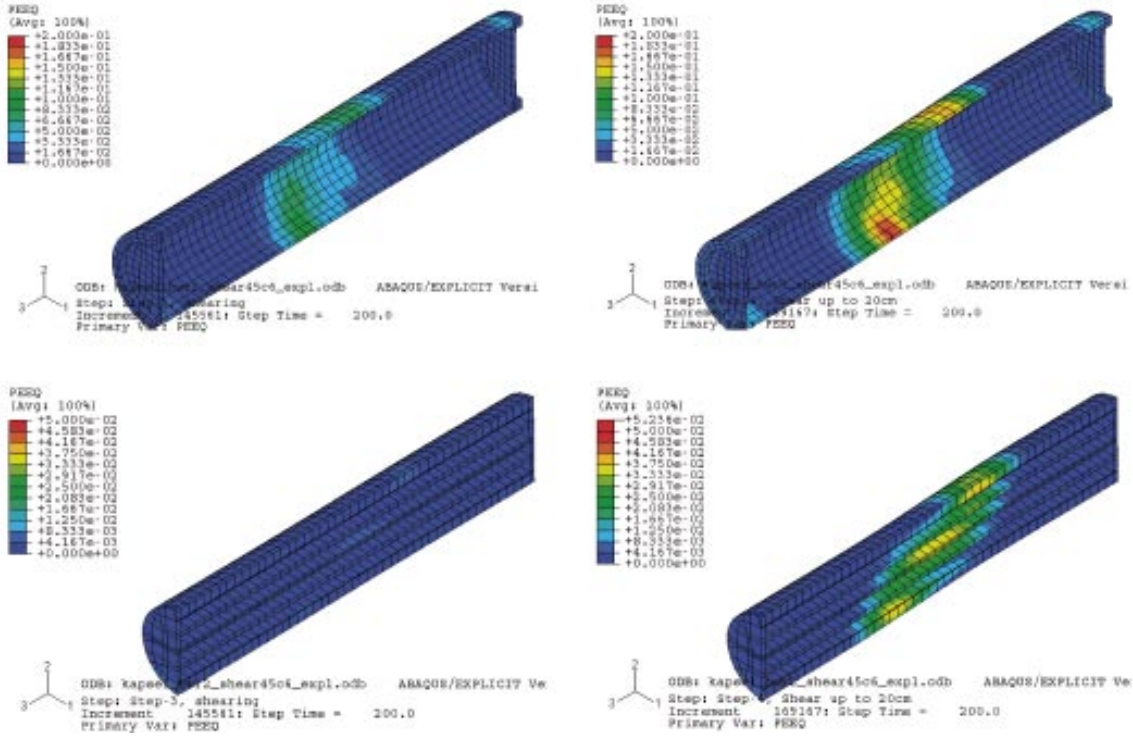

Figure 4-5. *Shear 45c6; Ca-bentonite; ρ_m = 2,050 kg/m³; 45° tension shear. Plastic strain in the copper and steel parts after 10 cm and 20 cm displacement.*

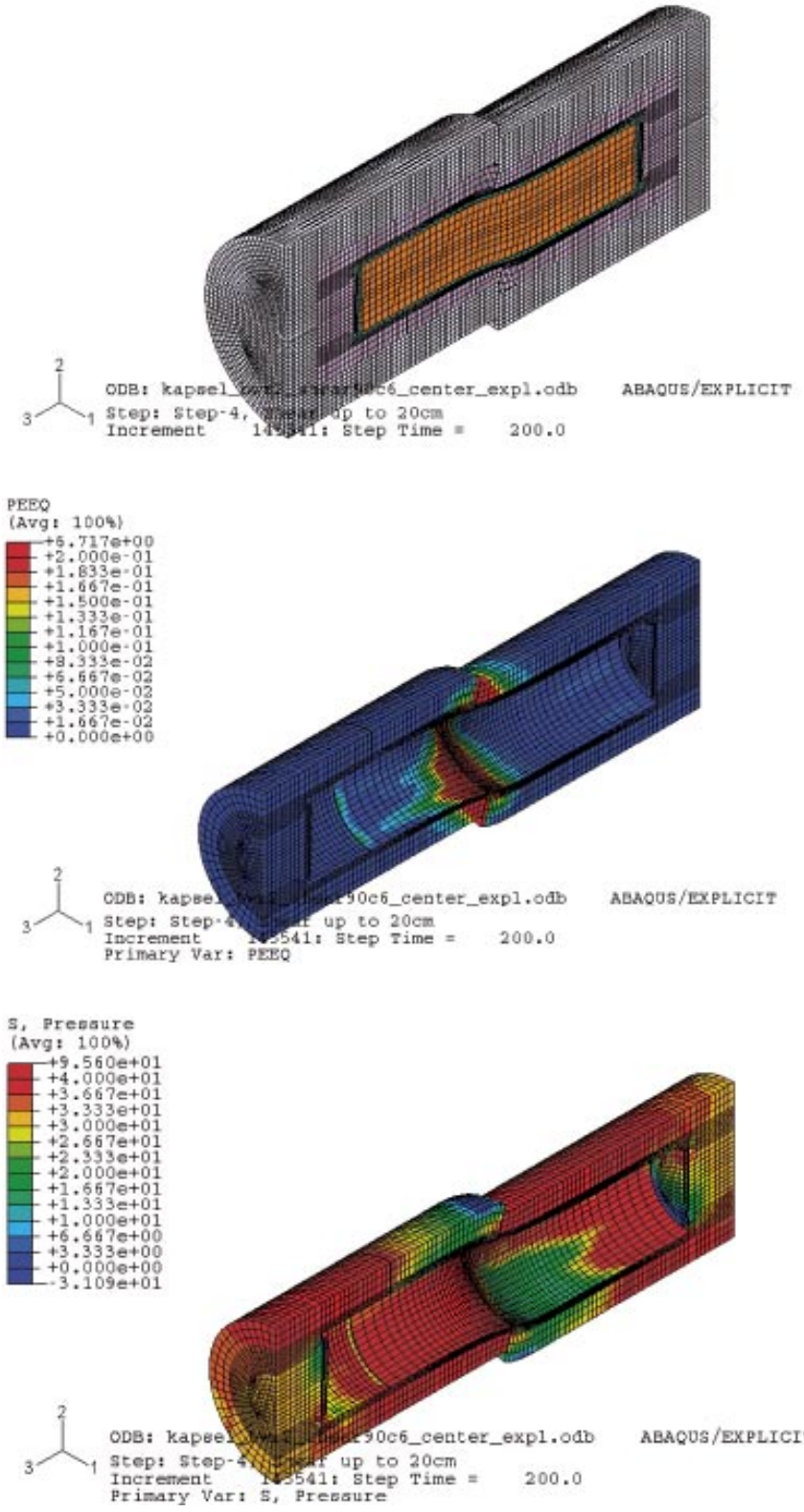

Figure 4-6. *Shear 90c6_c; Ca-bentonite; ρ_m = 2,050 kg/m³; 90° centric shear. Results after 20 cm shear. Deformed entire mesh, plastic strain and average stress (MPa) in the bentonite.*

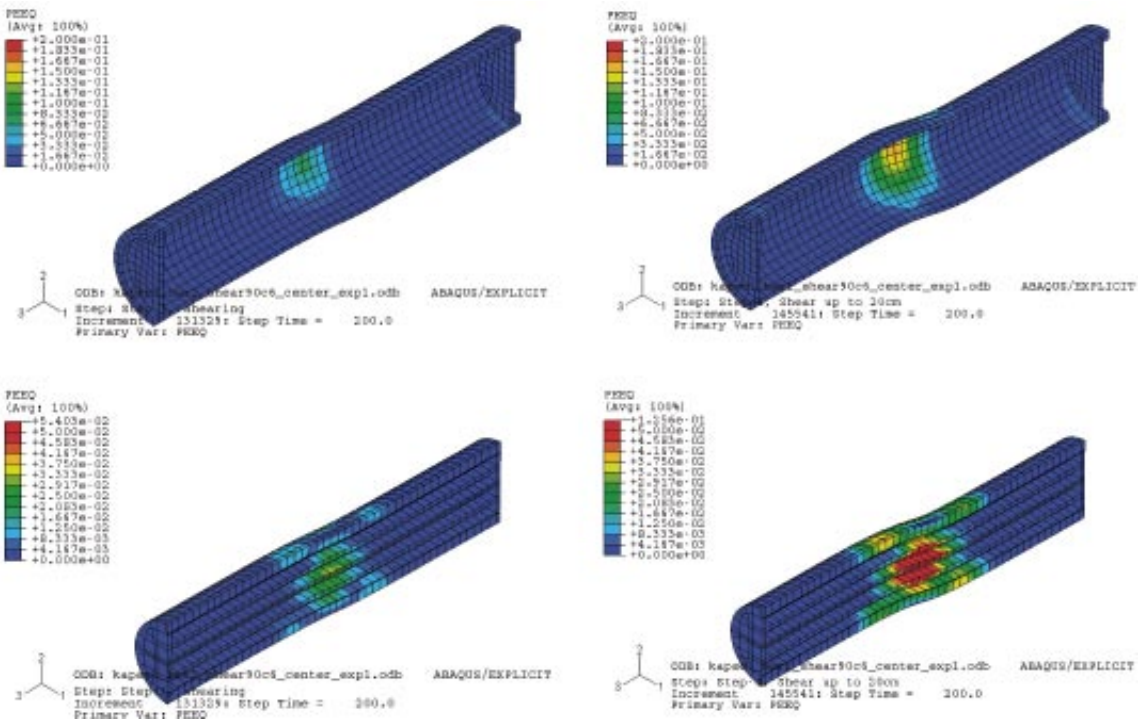

Figure 4-7. *Shear 90c6_c; Ca-bentonite; ρ_m = 2,050 kg/m³; 90° centric shear .Plastic strain in the copper and steel parts after 10 cm and 20 cm displacement.*

Figures 4-8 and 4-9 show the results of calculation *Shear 22c8* where tension shear at the inclination 22.5° occurs through a deposition hole filled with Ca-bentonite with the density 2,050 kg/m³. The effect on the buffer resembles the results from *Shear 45c6* (Figure 4-3) but the zone with plastic strain >5% is wider and covers a large part of the buffer between the canister and the rock as well as at the lids. The plastic strain in the copper and steel is as a consequence of the large plastication of the buffer smaller with a maximum that is about half of the maximum for the 45° case or about 10% for the copper and 2% for the steel after 20 cm shear.

The difference between tension shear and compression shear is illustrated by the results from calculations *Shear 22c6* and *Shear 22c8* shown in Figure 4-10. The deformed copper canister and the plastic strain in the copper canister are shown for the two cases when shear occurs at the inclination 22.5° through a deposition hole filled with Ca-bentonite with the density 2,050 kg/m³. The difference between tension shear and compression shear is very obvious both regarding deformations and plastic strain. The deformation plot (with deformation magnification of 5) shows that the canister logically is elongated in the case of tension shear while it is compressed in the case of compression shear. Also the deformation of the lids differs a lot since they are bowl shaped in the case of tension while they are squashed flat in the case of compression. The plastic strain differs a lot as well. In the case of tension the plastic strain is large in a major part of the copper tube with a maximum of about 10% while in the case of compression shear the plastic strain is low in the copper tube and very high at the flanges of the lid (up to 32%).

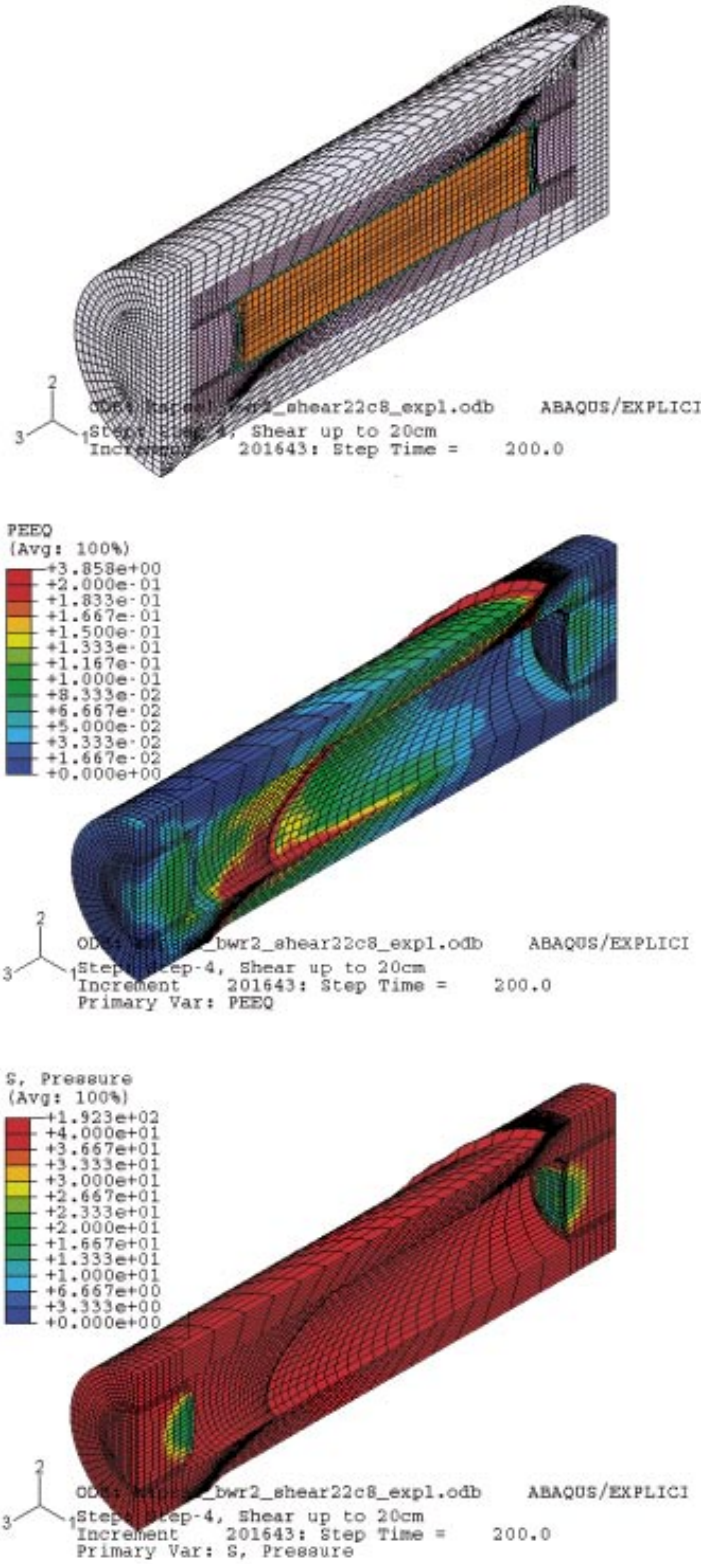

Figure 4-8. *Shear 22c8; Ca-bentonite; ρ_m = 2,050 kg/m^3; 22.5° tension shear. Results after 20 cm shear. Deformed entire mesh, plastic strain and average stress (MPa) in the bentonite.*

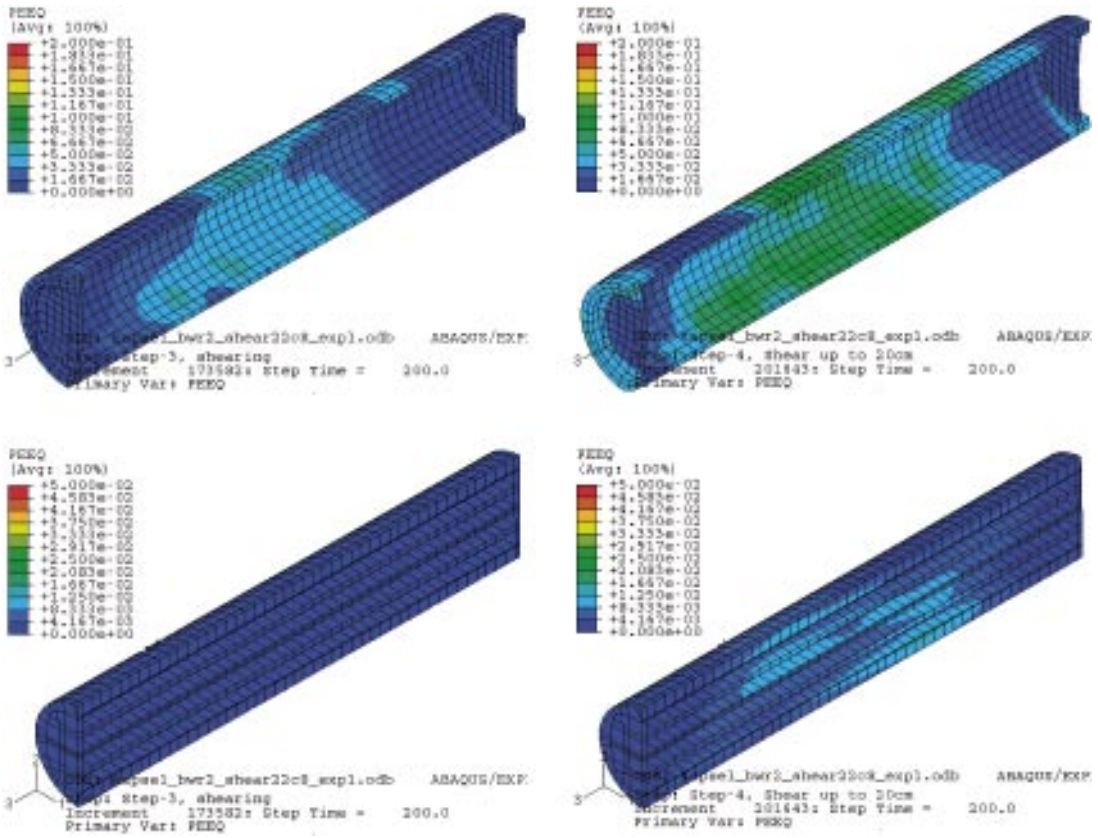

Figure 4-9. *Shear 22c8; Ca-bentonite; ρ_m = 2,050 kg/m³; 22.5° tension shear. Plastic strain in the copper and steel parts after 10 cm and 20 cm displacement.*

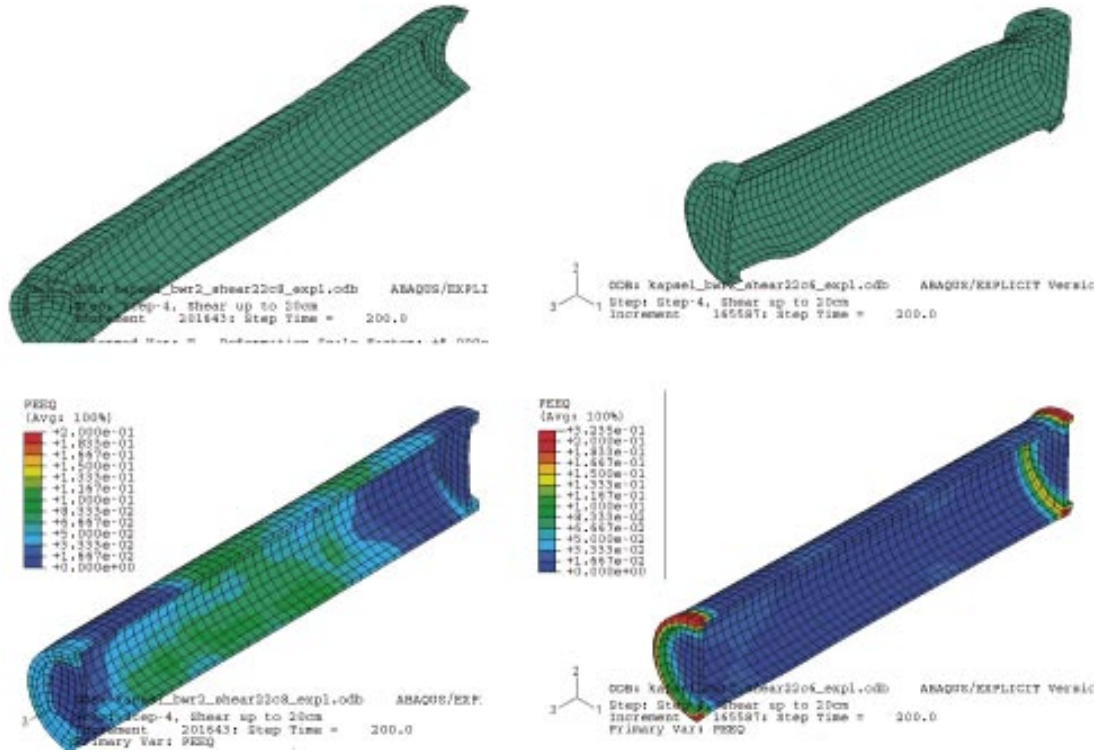

Figure 4-10. *Ca-bentonite; ρ_m = 2,050 kg/m³; 22.5° shear. Comparison between tension and compression shear. The upper left figure shows the deformed copper canister at tension and the upper right figure at compression (displacement magnification factor 5). The lower left figure shows the plastic strain in copper at tension and the lower right figure at compression.*

The difference between Ca-bentonite and Na-bentonite is illustrated in Figure 4-11. The deformed copper canister, the plastic strain in the copper and the plastic strain in the bentonite are shown for both materials for eccentric shear at the density 2,000 kg/m^3. The patterns are similar for the two materials but there are some important differences caused by the difference in stiffness and shear strength of the bentonites. The copper canister is much more deformed in the case of Ca-bentonite, which causes a much stronger plastic strain in the ¼ point of the copper tube but no obvious difference in the centre of the canister. The maximum plastic strain in the copper tube is 6.5% in the case of Ca-bentonite while it is only 2% in the case of Na-bentonite. However, in the lid the circumstances are quite the reverse with a maximum of 11% in the case of Na-bentonite and only about 7% in the case of Ca-bentonite. This latter difference is not easy to explain but may be due to that the bending is so strong in the tube that the stresses are lower in the lid.

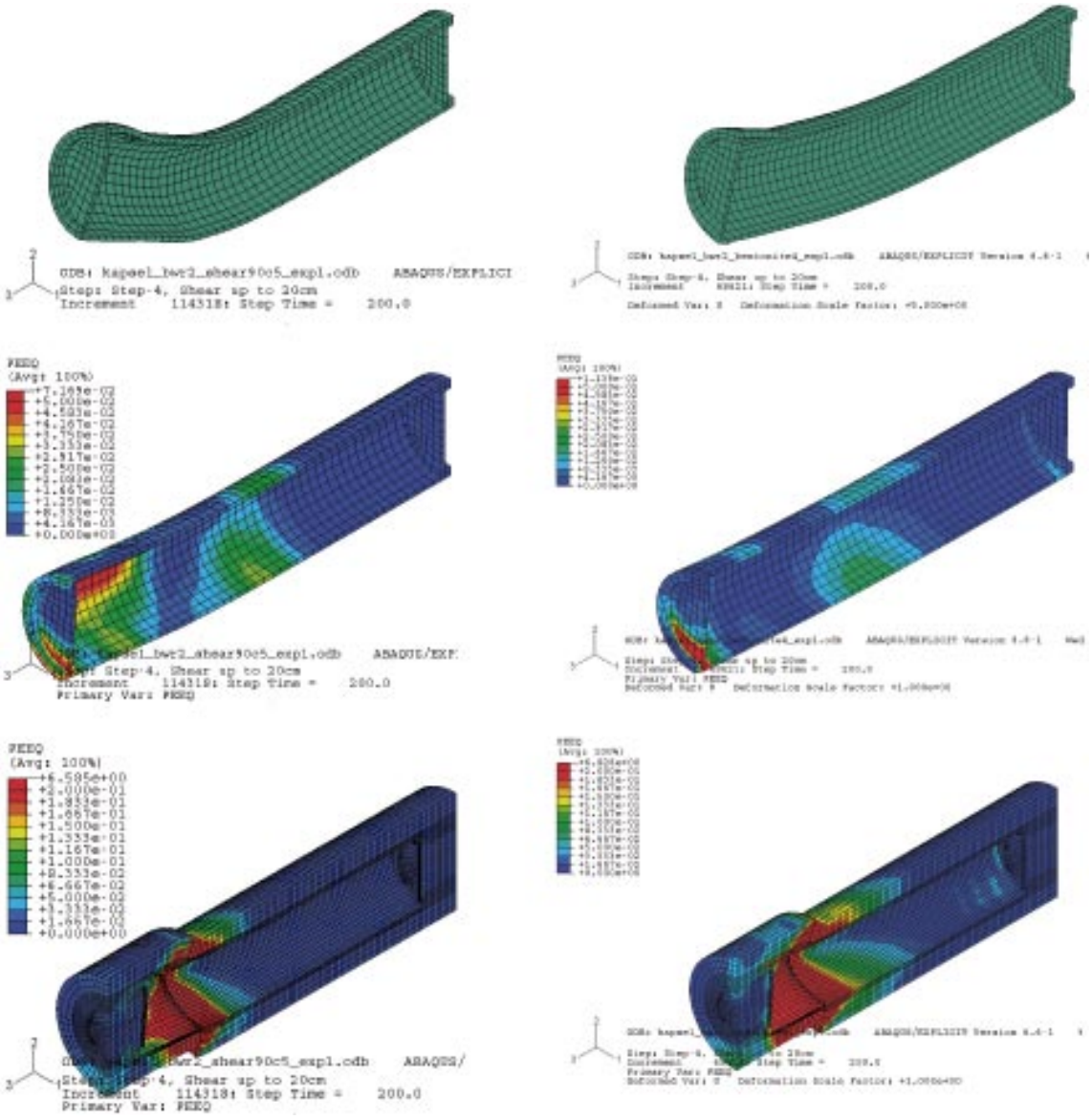

Figure 4-11. *Eccentric 90° shear at the density 2,000 kg/m^3. Comparison between Ca-bentonite (left figures) and Na-bentonite. The figures show (from top) the deformed copper canister, the plastic strain in the copper, and the plastic strain in the bentonite.*

Finally, the influence of the shear displacement is illustrated in Figure 4-12. The plastic strain in the copper and steel is shown after 10 and 20 cm in calculation *Shear 90c6* where eccentric shear with the inclination 90° towards the hole axis occurs through a deposition hole filled with Ca-bentonite with the density 2,050 kg/m^3. The influence of shear displacement is rather strong for this case. The plastic strain in the copper tube increases from maximum 5.5% at the shear displacement 10 cm to maximum 13.5% at 20 cm. In the steel the maximum plastic strain increases from 2.4% to 7% for corresponding cases.

It is not easy to find general trends due to all variations in parameters (bentonite type, bentonite density, shear angle, shear direction and shear plane location). The following observations can be noticed:

- Plastic strain larger than 1% was reached in the copper already at 10 cm shear in all cases with Na- and Ca-bentonite. However, for several cases of Na-bentonite and one case of Ca-bentonite such plastic strain was only reached in the lid.
- The maximum plastic strain in the copper tube and in the iron insert was for all cases larger for the Ca-bentonite than for the Na-bentonite. In the copper tube it was generally 2–5 times larger but even larger differences occur. The reason is of course that the Ca-bentonite is stiffer and has higher swelling pressure and strength than the Na-bentonite. The difference was illustrated in Figure 4-11.
- It is surprising that this is not valid for the lid. For at least half of the cases the plastic strain in the lid was smaller in the case of Ca-bentonite than Na-bentonite. The reason for this is not completely clear but it seems that the lid is more stressed the more it moves in the clay. If the tube is strongly plasticized and bent the canister lid will move less than if it is not bent, which thus results in lower stresses in the lid. This was also illustrated in Figure 4-11.
- A doubled shear displacement from 10 cm to 20 cm did not imply a doubling of the plastic strain in the copper tube for any of the cases with Na-bentonite with one or two exceptions. The increase in plastic strain was generally 20–50%. For the cases with Ca-bentonite the influence of the shear displacement was much stronger and a doubled displacement from 10 cm to 20 cm yielded for all cases an increase larger than 50% (with two exceptions) and for more than half of the cases a doubling or more. The latter was illustrated in Figure 4-12.

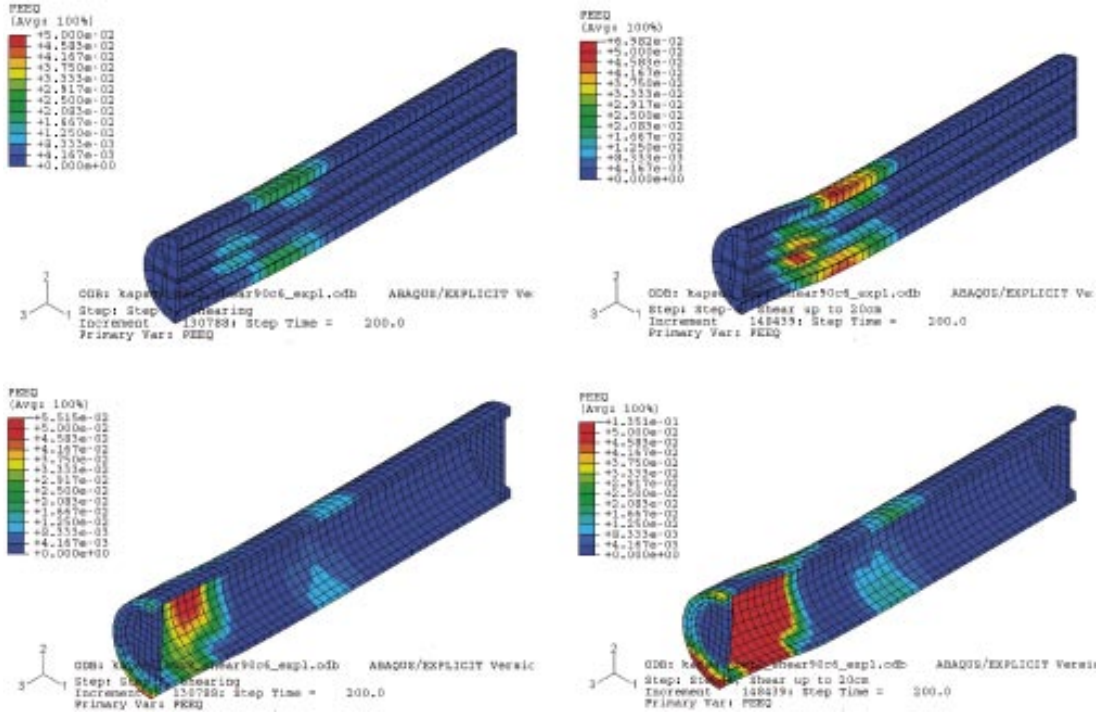

Figure 4-12. *Ca-bentonite, density 2,050 kg/m^3, eccentric shear. Comparison between the plastic strain in the steel and copper after 10 cm shear (left) and 20 cm shear. Same scales.*

The main reason for this difference is probably that Na-bentonite has lower stiffness and strength than Ca-bentonite, which means that the Na-bentonite will plasticize earlier and a larger part of the buffer will reach its peak shear resistance earlier. If the entire buffer is ideally plastic the magnitude of the shear displacement has very little influence on the canister damage since the canister "floats around" in the buffer.

- It is a little surprising that the shear inclination 45° was more harmful for the copper tube than the shear direction 90° when tension shear is considered. One would expect 90° to be worst since the momentum and the bending force are higher, but the tension shear at 45° seems to cause a tensile force on the canister tube that exceeds the effect of the bending force. The difference in maximum plastic strain in the copper tube between 45° tension shear and 90° shear with otherwise identical conditions was rather large for all cases except for Ca-bentonite with the density 2,050 kg/m^3. The latter cases are illustrated by Figures 4-5 and 4-7.
- Higher plastic strain in the copper tube was at the shear angle 90° reached at eccentric shear than at centric shear for all cases except the high density Ca-bentonite case. The reason is that at low buffer stiffness the canister tilts if there is not enough canister length (more than half the canister) to keep the canister in a firm grip, but at high buffer stiffness the length of half the canister is enough to prevent tilting.
- At the shear inclinations 45° and 22.5° tension shear was always more harmful for the copper tube than compression shear. The highest value 19% was reached after 20 cm shear in Ca-bentonite with the density 2,050 kg/m^3. Figure 4-10 illustrates the difference.
- The copper lid was for many cases more stressed than the copper tube. The maximum plastic strain in the copper lid was 32%, which was reached after 20 cm shear in Ca-bentonite with the density 2,050 kg/m^3 at compression shear and the shear angle 22.5° as shown in Figure 4–10. However, the plastic strain in the copper lid might be irrelevant since the high stresses are mainly occurring due to the jutting flange and the lid may be redesigned without such flange. In addition the element mesh may be too course for studying these stresses in detail.
- The plastic strain in the steel insert was rather large (>5%) for some cases of the high density Ca-bentonite but always smaller than the plastic strain in the copper as illustrated in, e.g. Figure 4-12. The reason is of course that plastization starts at much higher Mises stress in the steel (260 MPa) than in the copper (50 MPa).

For the cases with the shear angle 90° the high stiffness and high yield stress in the steel control the bending of the canister and thus also the plastic strain in the copper. Different yield strength of the steel will thus have a strong impact on the plastic strain in the copper. Different yield strength of the copper is not judged to have a strong impact since the strain is largely controlled by the steel. However, this is not necessarily valid for inclined tension shear since for these cases a large part of the strain originates from tension rather than from bending.

4.5 Uncertainties

The calculations are of course associated with several uncertainties of different kinds and degrees of seriousness.

Material model of buffer

There are some uncertainties regarding the material model. The prime one is the model of Ca-bentonite. The properties of Ca-bentonite have not been investigated to such extent as the properties of Na-bentonite. The model is based on the knowledge of Na-bentonite and a limited amount of tests on Ca-bentonite.

The influence of the rate of shear on the stiffness and strength of the bentonite is investigated with uniaxial tests with different deformation rates. The results are directly applied for the deformation rate 1 m/s. Locally the rates can be different and the model does not take this into account. However, this effect is judged to be small since it requires an order of magnitude difference in rate to yield a difference of 16% in strength.

The properties of the bentonite might change with time due to transformations or cementation. Such circumstances are treated in Chapter 5.

Material models of copper and steel

The properties of the copper and steel are taken from earlier tests and information. The yield properties of copper are very much dependant on how the copper has been processed. Since the magnitude of the plastic strain in the copper after a rock shear to large extent is dependant on the yield properties it is important to make tests on the actual material in the canister. If new information and test results emerge it might be necessary to re-evaluate the calculations.

Contact elements

The contact elements between the bentonite and the rock or the canister have been assigned the same properties with a friction angle that is valid for smooth surfaces /7/ and no cohesion. If the surface is rough, which could be the case for the rock or a chemically affected copper surface, the friction angle could be higher. However, this property is not judged to have a significant influence on the results. The cohesion has been assumed to be zero, which means that the buffer does not stick to the rock or canister if there are tension stresses between the surfaces. This plausible assumption needs to be checked.

Geometry and element mesh

The element mesh could be too coarse to reveal local stress concentrations, especially in the lids. The geometry of the lids does not agree with the present design. If these matters are important some checks should be made by using a more refined mesh and updated lid geometry.

Inhomogeneities in the buffer

The buffer is assumed to be completely homogeneous with a density corresponding to the expected average density of the buffer. In reality the buffer has a slightly lower density close to the canister and close to the rock and thus a slightly higher density in the rest of the buffer due to the slots that exist from start. During wetting the buffer swells and homogenises but after long time there are still differences in density especially in radial direction due to the friction in the bentonite. The buffer is thus softer close to the rock and buffer and stiffer in the remaining parts, which affects the consequences of a rock shear. However, the influence of this difference is judged to be small.

5 Influence of buffer transformation

5.1 Introduction

Chemical transformation of the buffer may occur and will change the mechanical properties of the buffer. In this chapter two types of transformations will be analysed, namely illitization and cementation. Such transformations are not likely to occur /8/ but it is anyway valuable to have an idea of possible consequences of a transformation. A problem is that the properties of the transformed bentonite are not known in detail, so "intelligent guesses" and the assumption that the material behaves like similar natural materials have to be used.

5.2 Transformation to illite

General

Transformation to illite involves an almost complete loss in swelling properties if all the smectite is transformed. The analysis will assume a complete transformation but of course all variants between this extreme and no transformation at all are possible. According to Karnland and Birgersson /8/, the swelling pressure, which is the decisive property, will decrease as a function of the lost smectite content. All cases of partly illitization will thus yield effects between these extremes.

Material model

The base parameters of the required material model for the rock shear are the swelling pressure, the shear strength (actually stress-strain relation during shear) and the influence of the shear rate on the shear strength. The shear strength of non-cemented compressible clay can be estimated from the swelling pressure and the friction angle.

The actual properties of smectite transformed to illite are not known and may be related to the processes involved in the transformation (collapse of inter-lamellar layers, Si-precipitation, cementation etc.). An example of a resulting material is an illite that resembles the illite represented by Swedish illitic post glacial clays. Some unreported tests on such materials were performed in the early 80-ies. An illite from Skå-Edeby (liquid limit 50–60%) was dried, ground and compacted to samples with different densities. The samples were saturated with tap water and some properties were measured. The swelling pressure was measured and the results are shown in Figure 5-1.

The figure shows that the swelling pressure at buffer densities is between 100 kPa and 1,000 kPa. No test of shear strength was done but experiences from similar materials indicate a friction angle of 30–40°. The deviatoric stress at failure can be estimated with Equation 5-1.

$$q_f = 2p\sin\varphi \qquad (5\text{-}1)$$

where

q_f = deviatoric stress at failure

p = average effective stress (swelling pressure)

φ = friction angle

Table 5-1 shows evaluated deviatoric stress at failure for different densities assuming a friction angle of 40 degrees and no cohesion. The influence of shear rate is not known but similar influence as for MX-80 has been assumed.

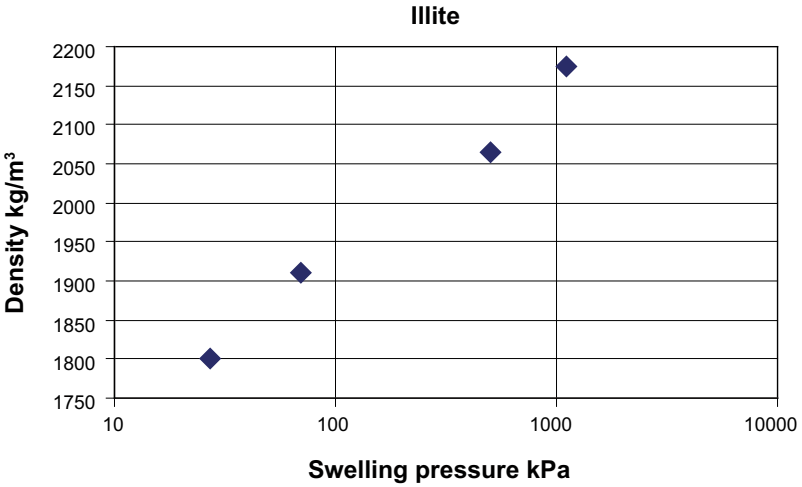

Figure 5-1. *Measured swelling pressure of the illite tested as a function of the density at saturation.*

Table 5-1. Evaluated deviatoric stress at failure for an illitic clay and comparison with MX-80.

Case no	ρ_m (kg/m³)	p (kPa)	q_f (kPa) at low shear rate	q_{fs} (kPa) at v_s = 1 m/s	q_{fs} (kPa) used for MX-80
1	1,950	130	167	330	3,900
2	2,000	200	257	510	6,000
3	2,050	350	450	900	10,000
4	2,100	550	707	1,400	15,200

ρ_m = density at saturation.

p = swelling pressure derived from Figure 5-1.

q_f = deviator (Mises) stress at failure derived from Equation 5-1.

q_{fs} = deviator (Mises) stress at failure corrected for shear rate.

v_s = shear rate.

Effect of rock shear

Table 5-1 shows that the strength of the illitic clay is only a tenth of the strength of MX-80, which clearly indicates that the effect on the canister of a rock shear is insignificant compared to when no transformation has taken place. The reason for the low strength is of course the low swelling pressure of the illite. All cases of partly illitization can be concluded to lead to consequences of a rock shear that are less severe than if no transformation takes place due to the loss in swelling pressure.

Comments

This simple evaluation is based on laboratory tests on natural illitic clay. The actual behaviour of a smectite transformed to illite is not known, but the basic observation that the shear strength is low due to the low swelling pressure must be valid also for transformed clay. Thus, the effect of a rock shear is not expected to be a problem if the transformed illitic clay has properties resembling natural compressible clays with low cohesion and a friction angle. However, if the clay is cemented it may have a very high cohesion, which strongly will influence the effect of

a rock shear. The properties of such a material are not known, but the consequences will probably be severe for the buffer in many other respects than a rock shear. The effect of a rock shear through a partly cemented buffer is treated in the next section.

5.3 Cementation of parts of the buffer

General

Any transformation of the buffer that can cause parts of the buffer to be cemented could be critical at a rock shear if the properties of the cemented parts are unsuitable. Since neither the processes nor the properties are known several assumptions have been made. Only one calculation has been done and all uncertainties yield that the results must be considered to be an example of what could happen rather than a proper analysis.

One factor that can enhance the transformation processes is the temperature so it has been assumed in the calculation that only a region with the thickness 8.75 cm around the canister has been cemented.

The calculation has used the reference calculation with the buffer material Na-bentonite at the density at saturation 2,000 kg/m^3 as base and comparison can thus be made between the cement-calculation and the reference calculation without any cementation.

Element mesh

The element mesh used for the calculation is shown in Figure 5-2. The mesh is identical to the mesh used for calculation *Shear 90c1* with the exception that the innermost four elements around the canister have been assigned properties of cemented bentonite. The extent (thickness) of the cemented part is a ¼ of the buffer that is 8.75 cm. Eccentric shear at 90° shear angle has been modelled.

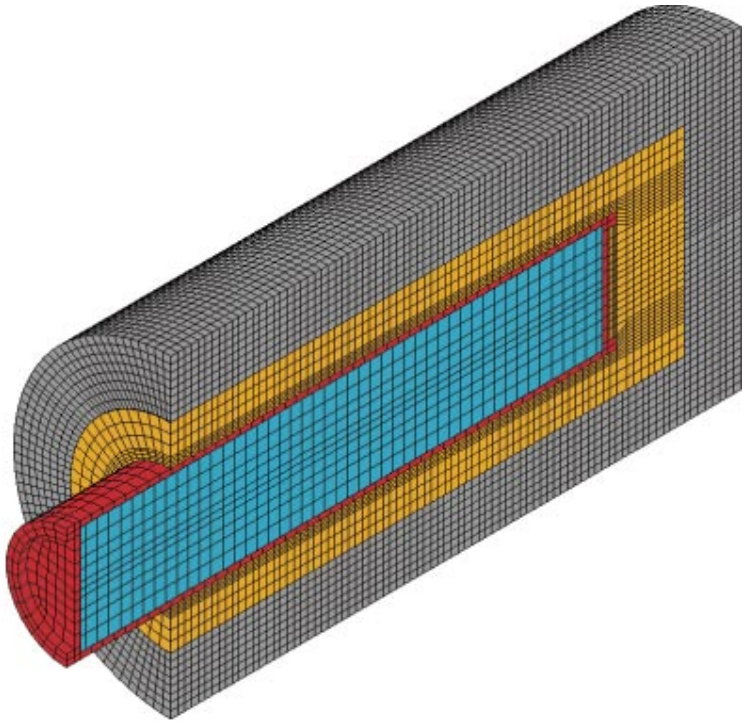

Figure 5-2. *Part of the element mesh used for the calculation of a rock shear through partly cemented buffer. The four thin elements close to the canister represent cemented buffer with the thickness 8.75 cm.*

Material model

The Material model of cemented buffer is described in Section 3.2.3. The input data are chosen with the assumption that the cemented bentonite has completely lost its swelling pressure and has properties that resemble rather poor cement but still are probable. The material model includes effect of unloading and reloading as well as tension. Those parts are included but are not likely to be active due to the stress paths expected at a rock shear. Only the compression properties will be shown in this chapter.

Table 5-2 shows the basic properties of the cemented and natural unaffected bentonite including the swelling pressure p and the Mises stress at failure q_{fs} at the shear rate v_s = 1 m/s.

Table 5-3 shows the elastic and plastic properties at compression.

Results

Only one calculation (*Cement5h*) has been performed. It was rather difficult to make it converge for 20 cm displacement. Figures 5-3 and 5-4 show examples of results. Figure 5-3 shows the deformed mesh after 20 cm shear. The figure of the cemented bentonite shows that some much stressed elements have been strongly deformed (degenerated).

Figure 5-4 shows the deformed copper and the plastic strain in the copper and steel. The same figures from the calculations of un-cemented Na-bentonite (*Shear 90c1*) are included for comparison. The comparison shows that the difference between the calculations is rather small but the cemented bentonite yields a little higher stresses in the canister. Especially the local area close to the shear plane where some elements degenerated shows a strong increase in plastic strain for the cemented bentonite case.

Table 5-4 shows the maximum plastic strain in the copper and steel and a comparison with the un-cemented case. Both the copper tube and the steel are subjected to 20–60% larger maximum plastic strain in the case of cemented bentonite, although the case is the opposite in the lid of the copper. The results seem logical, since the cemented buffer is a little stiffer than the natural bentonite. The reverse effect for the lid is also in agreement with the earlier observations when comparing Ca-bentonite with Na-bentonite and can probably be explained in the same way.

Table 5-2. Basic properties of the cemented and un-cemented bentonite.

Material	ρ_m kg/m³	e	p MPa	q_{fs} at v_s = 1.0 m/s MPa
Na-bentonite	2,000	0.78	6.1	6.0
Cemented bentonite	2,000	0.78	0	30.0

Table 5-3. Elastic properties and yield curve of the cemented and un-cemented bentonite.

Mtrl	Elastic part		Plastic part: Compression hardening[2] (MPa) at the specified plastic strain ε_p[3] (%)												
	E[1]	v	0	0.2	0.5	0.9	1.0	1.3	1.8	2.0	2.3	5.0	10	20	30
Na-b	.363	0.49	3.63	4.85	5.57	5.95		6.19	6.3		6.22				6.22
Ce-b	36.3	0.3	25				30			20		2	0.1	0.01	0.01

1) GPa.

2) Rows 3 and 4.

3) Row 2.

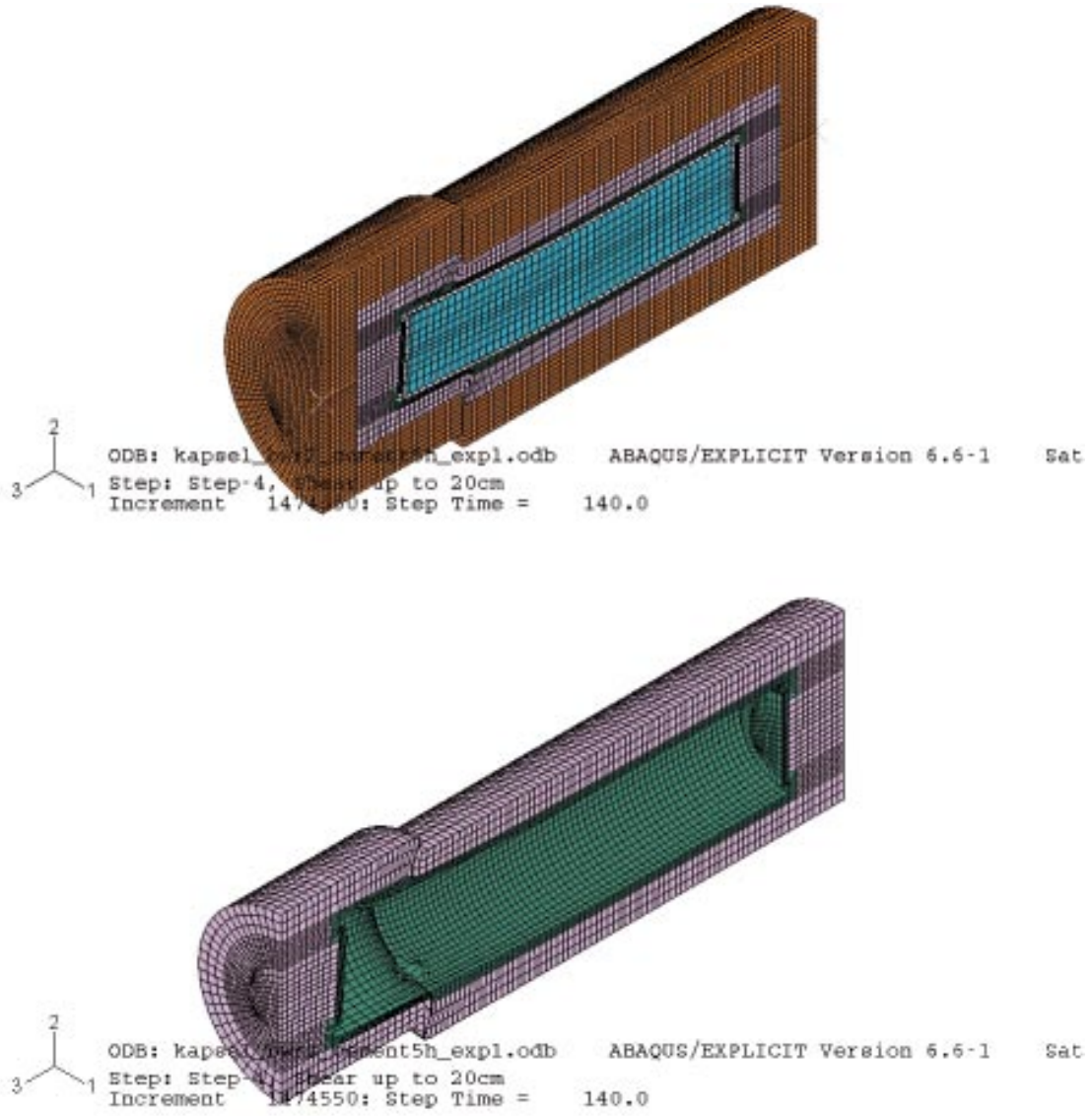

Figure 5-3. *Rock shear through partly cemented bentonite. The entire deformed mesh (upper) and the deformed mesh of the unaffected and cemented bentonite after 20 cm shear displacement are shown.*

Table 5-4. Plastic strain in the canister after a rock shear with cemented buffer (*Cement5h*) and comparison with the un-cemented case (*Shear 90c1*).

Calculation	ρ_m kg/m^3	Shear angle °	Shear direction/ location	Maximum plastic strain (%) After 10 cm shear			After 20 cm shear		
				Cu-tube	Cu-lid	Fe-insert	Cu-tube	Cu-lid	Fe-insert
Shear 90c1	2,000	90	excentr.	1.2	7.9	<1	2.0	11	1.7
Cement5h	2,000	90	excentr.	1.6	6.7	1.2	2.5	8	2.8

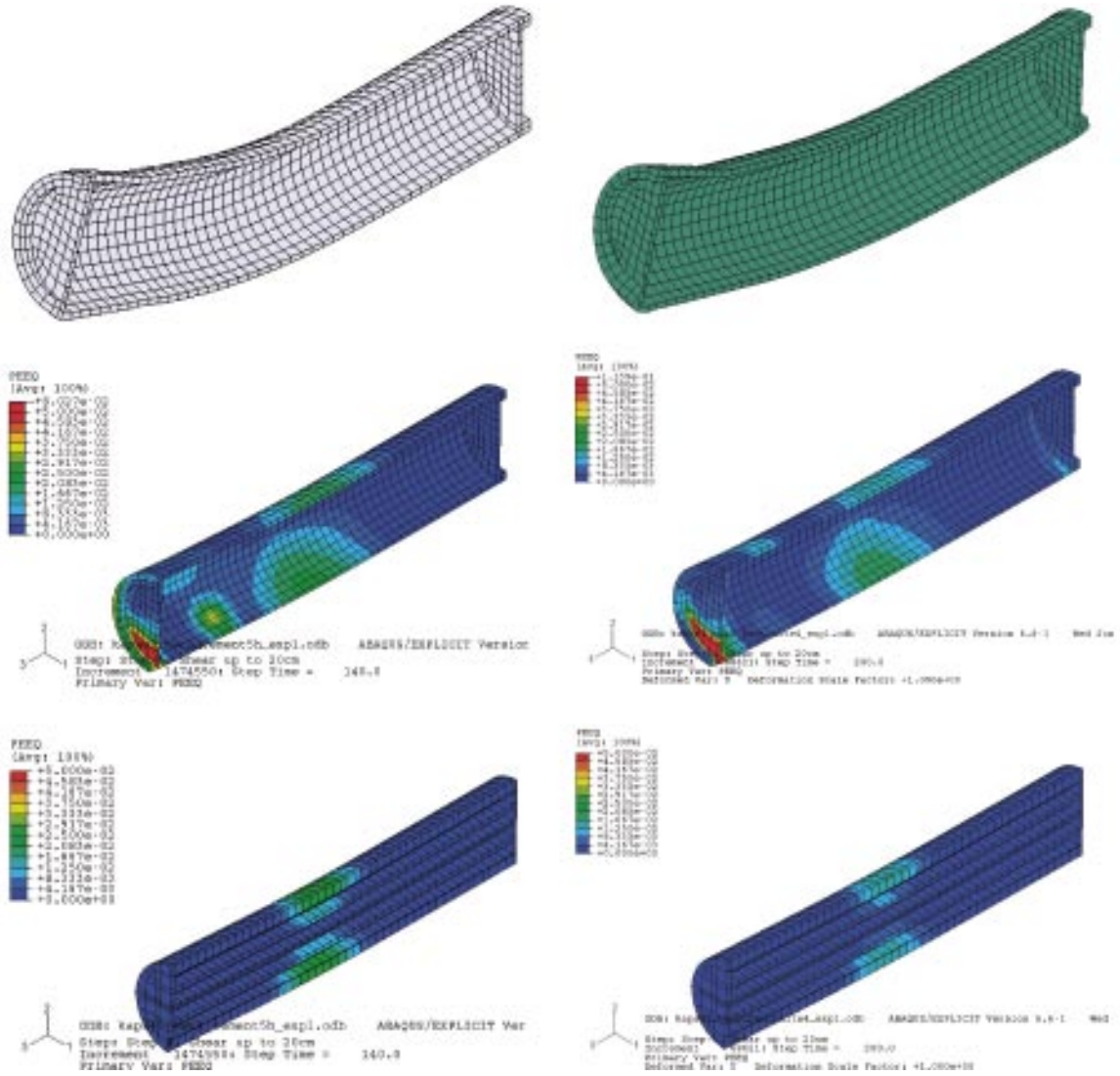

Figure 5-4. *Comparison of results of a 20 cm eccentric rock shear through un-cemented Na-bentonite and partly cemented Na-bentonite. The left figures show the results from partly cemented bentonite (Cement5h) while the left are results from not cemented bentonite (Shear 90c1). The upper figures represent the deformed copper canister with the displacement magnification 5, the middle figures represent the plastic strain in the copper and the lower figures represent the plastic strain in the steel.*

Conclusions and comments

The example calculation shows that the damaging effect on the copper and steel is stronger when a limited amount of bentonite around the canister is partly cemented compared to the case of no cementation. The reason is that the cemented bentonite has been assigned properties that yield a stiffer material although there is no swelling pressure. The properties of the cemented buffer seem reasonable according to present knowledge but the uncertainty of the actual properties is of course a major drawback of the calculation, which thus must be considered an example rather than a prediction.

The effect of a rock shear on the canister is in this example not so strong that it jeopardizes the function of the canister, but if it cannot be excluded that the cemented bentonite is much stiffer or that a much larger part of the buffer is cemented the canister may be severely damaged.

6 Conclusions

The effect on the canister of an earthquake induced 20 cm rock shear with the shear rate 1 m/s through a deposition hole has been investigated for a number of different shear cases and for different properties of the buffer material. The influence of mainly the following factors has been investigated:

1. The inclination of the intersection between the shearing fracture and the deposition hole axis.
2. Shear direction when the inclination deviates from 90°.
3. The location of the shear plane when the inclination is 90°.
4. The magnitude of the shear displacement.
5. Bentonite type.
6. Bentonite density.
7. Transformation of the buffer to illite or cemented bentonite.

The results from the calculations show that all these factors have important influence on the damage of the canister but the influence is for most factors not easily described since there are mutual interferences between the different factors. The following general trends regarding the first six factors can be perceived:

- Plastic strain larger than 1% was reached in the copper already at 10 cm shear in all cases with Na- and Ca-bentonite. However, for several cases of Na-bentonite and one case of Ca-bentonite such plastic strain was only reached in the lid.
- The plastic strain in the steel was generally lower than in the copper mainly due to the higher yield stress in the steel. For all cases of Na-bentonite except one and for about half of the Ca-bentonite the plastic strain was lower than 1% after 10 cm shear.
- The shear inclination 45° was more harmful for the copper tube than the shear direction 90° when tension shear is considered. Tension shear at 45° seems to cause a tensile force on the canister tube that exceeds the effect of the bending force. The difference in maximum plastic strain in the copper tube between 45° tension shear and 90° shear with otherwise identical conditions was rather large for all cases except for Ca-bentonite with the density 2,050 kg/m^3.
- At the shear inclinations 45° and 22.5° tension shear was always more harmful for the copper tube than compression shear. The highest value 19% was reached after 20 cm shear in Ca-bentonite with the density 2,050 kg/m^3.
- Larger plastic strain in the copper tube was at the shear angle 90° reached at eccentric shear than at centric shear for all cases except the high density Ca-bentonite case. The reason is that at low buffer stiffness the canister tilts if there is not enough canister length (more than half the canister) to keep the canister in a firm grip, but at high buffer stiffness the length of half the canister is enough to prevent tilting.
- The plastic strain increased logically with increasing shear displacement although the influence of the shear displacement is reduced the softer the buffer material is. A doubled shear displacement from 10 cm to 20 cm did not imply a doubling of the plastic strain in the copper tube for any of the cases with Na-bentonite with one or two exceptions. The increase in plastic strain was generally 20–50%. For the cases with Ca-bentonite the influence of the shear displacement was much stronger and a doubled displacement from 10 cm to 20 cm yielded for almost all cases an increase larger than 50% and for more than half of the cases a doubling or more. The main reason for this difference is probably that Na-bentonite has lower stiffness and strength than Ca-bentonite, which means that the Na-bentonite will

plasticize earlier and a larger part of the buffer will reach its peak shear resistance earlier. If the entire buffer is ideally plastic the magnitude of the shear displacement has very little influence on the canister damage since the canister "floats around" in the buffer

- The maximum plastic strain in the copper tube and in the iron insert was for all cases larger for the Ca-bentonite than for the Na-bentonite. In the copper tube it was generally 2–5 times larger but even larger differences occurred. The reason is of course that the Ca-bentonite is stiffer and has higher swelling pressure and strength than the Na-bentonite.
- For the same reason the plastic strain is of course larger the higher the density of the buffer is.

Geochemical transformation of the buffer can lead to a material with quite different properties than the original buffer. The effect of a rock shear through such a buffer may of course have rather different consequences than through the original buffer.

- The analysis of the effect of conversion to illite yielded that the effect on the canister of a rock shear is insignificant compared to when no transformation has taken place since the strength of the illitic clay is only a tenth of the strength of MX-80. The reason for the low strength is of course the low swelling pressure of the illite. All cases of partly illitization can be concluded to lead to consequences of a rock shear that are less severe than if no transformation takes place due to the loss in swelling pressure.
- Cementation of bentonite with the thickness 8.75 cm around the canister yields that the effect of a rock shear is more severe than if the original bentonite is kept due to the increased stiffness of the buffer. However, the properties of cemented bentonite are not known so the calculation must be regarded as an example rather than as a prediction.

The calculations are associated with several uncertainties that should be considered when the consequences of a rock shear are analyzed.

- Besides the fact that the properties of the cemented buffer are not known, there are some uncertainties regarding the material models of the unaffected buffer. The prime one is the model of Ca-bentonite. The properties of Ca-bentonite have not been investigated to such extent as the properties of Na-bentonite. The model is based on the knowledge of Na-bentonite and a limited amount of tests on Ca-bentonite.
- The properties of the copper and steel are taken from earlier tests and information. Since the yield properties are of major importance for magnitude of the plastic strain the results of the calculations should be re-evaluated if new data emerge.
- The contact elements surrounding the buffer are assumed to have no cohesion at tensile stress, which should be checked.
- The element mesh could be too coarse to reveal local stress concentrations, especially in the lids. The geometry of the lids does not agree with the present design. If these matters are important some checks should be made by using a more refined mesh and updated lid geometry.
- The buffer is assumed to be completely homogeneous with a density corresponding to the expected average density of the buffer. In reality the buffer has a slightly lower density close to the canister and close to the rock and thus a slightly higher density in the rest of the buffer due to the slots that exist from start. However, the influence of this difference is judged to be small.

References

/1/ **Börgesson L, Hökmark H, Karnland O, 1988.** Rheological properties of sodium smectite clay. SKB TR 88-30. Svensk Kärnbränslehantering AB.

/2/ **Börgesson L, 1986.** Model shear tests of canisters with smectite clay envelopes in deposition holes. SKB TR 86-26. Svensk Kärnbränslehantering AB.

/3/ **Börgesson L, 1988.** Modelling of buffer material behaviour. Some examples of material models and performance calculations. SKB TR 88-29. Svensk Kärnbränslehantering AB.

/4/ **Börgesson L, 1992.** Interaction between rock, bentonite buffer and canister. FEM calculations of some mechanical effects on the canister in different disposal concepts. SKB TR 92-30. Svensk Kärnbränslehantering AB.

/5/ **Börgesson L, Johannesson L-E, Hernelind J, 2004.** Earthquake induced rock shear through a deposition hole. Effect on the canister and the buffer. SKB TR-04-02. Svensk Kärnbränslehantering AB.

/6/ ABAQUS Manuals. ABAQUS Inc.

/7/ **Börgesson L, Johannesson L-E, Sandén T, Hernelind J, 1995.** Modelling of the physical behaviour of water saturated clay barriers. Laboratory tests, material models and finite element application. SKB TR-95-20. Svensk Kärnbränslehantering AB.

/8/ **Karnland O, Birgersson M, 2006.** Montmorillonite stability – With special reference to KBS-3 conditions. SKB TR-06-11. Svensk Kärnbränslehantering AB.